4.3.4 Comets

RITA SCHULZ AND GIAN-PAOLO TOZZI

4.3.4.1 Mechanical data

Number of comets, comet reservoirs

Three comet reservoirs have been identified to date. The Oort cloud [50O] is composed of some 10^{11} - 10^{12} comets surrounding the Solar System at a distance of 2×10^4 - 10^5 AU. The Edgeworth-Kuiper belt [43E, 49E, 51K] (sometimes referred to as the Kuiper belt) and the scattered comet disk are reservoirs beyond Neptune. The Edgeworth-Kuiper belt is a thick torus between ~ 35 - 50 AU, centred around the ecliptic, and the scattered disk is composed of bodies with highly eccentric orbits. Reviews about Oort cloud and Edgeworth-Kuiper belt formation, structure and dynamics can be found in [04D1, 04M].

Marsden and Williams's catalogues [05M1] contains 2,221 observed comets, 1,880 are long-period (LP) comets (orbital period $P > 200$ a), 341 are *periodic* (P < 200 a). The orbital parameters of comets are also maintained and regularly updated on-line.

The official site is: www.cfa.harvard.edu/iau/Ephemerides/Comets/. Another on-line source is: ssd.jpl.nasa.gov. Both sites offer also the possibility to generate ephemeris of individual comets.

Although interstellar comets may exist, no comet on a clearly interstellar heliocentric directory has been observed.

Orbital charateristics

The orbit of a comet is completely defined by six parameters. The semi-major axis (a), the eccentricity (e), and the orbital period (P) determine the orbit characteristics. The inclination of the orbit (i), the argument of perihelion (ω) and the longitude of the ascending node (Ω) describe the orientation of the orbit in space with respect to the ecliptic. Sometimes the perihelion distance (q) is given instead of semi-major axis or eccentricity, and/or the longitude of the perihelion ($\varpi = \omega + \Omega$) replaces the argument of perihelion (ω). The time (τ) of perihelion passage is required for determination of the comet position at a certain epoch.

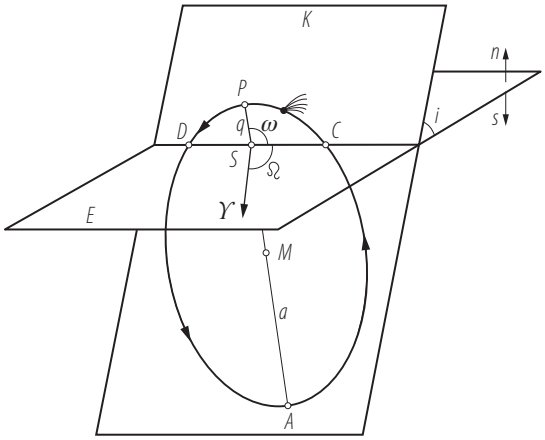

Fig. 1. The orbit of a comet: Orbit and the plane of ecliptic

Comet Taxonomy

Classification of comets on the basis of their dynamical properties has much improved in recent years. The original simple scheme of classifying comets according to their orbital period was revised, as backward numerical integration has shown that comets could change their orbital period. Comets are nowadays classified by their Tisserand parameter (originally introduced [87C]), which is a measure of the

influence of Jupiter on the comet dynamics and does not change significantly during the lifetime of a comet. The Tisserand parameter, T, is defined as:

$$T = \frac{a_J}{a} + 2\sqrt{\frac{a}{a_J}\times\left(1-e^2\right)}\cos(i)\,, \tag{1}$$

where a_J is the semimajor axis of Jupiter and a, e, and i refer to the comet orbit.

This parameter is an approximation of the Jacobi constant, the integral of the motion in a circular restricted three-body problem. It also gives the relative velocity of the object with respect to Jupiter during a close encounter: $V_0 = V_J\sqrt{(3-T)}$, with V_J being the orbital velocity of Jupiter. Objects with $T > 3$ cannot cross the Jupiter orbit in the circular restricted case, hence their orbit is either inside or outside the orbit of Jupiter.

Comets with $T < 2$ originate mainly from the Oort cloud. They are classified as nearly-isotropic comets, because their inclination, has a more or less isotropic distribution. Comets with $T > 2$ have their origin in the Edgeworth-Kuiper belt or the scattered disk and are classified as ecliptic comets, because they have very small inclinations. The ecliptic comets are sub-divided in three groups: (1) Jupiter family comets ($2 < T < 3$) have a strong gravitational interaction with Jupiter; (2) Encke-type comets ($T > 3$, $a < a_J$) have orbits entirely interior to Jupiter; (3) Chiron-type comet or Centaurs ($T > 3$, $a > a_J$) have orbits entirely exterior to that of Jupiter. Overviews of comet taxonomy based on Tisserand parameter are given in [96L2, 04D2].

Non-gravitational forces

Asymmetric sublimation produces a non-gravitational force on the comet nucleus that introduces an acceleration or deceleration (depending of the rotational direction of the nucleus) into the comet's motion. Proper modelling of these so-called non-gravitational perturbations is vital for correct orbit determination. Recent review in [04Y].

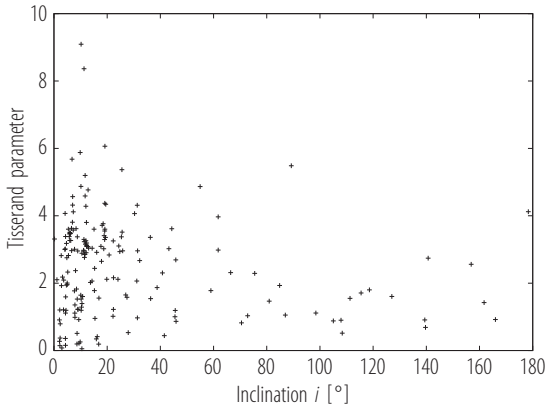

Fig. 2. The Tisserand parameter as a function of inclination for comets in Table 1 with $T > 0$ and $i < 1808$.

Table 1. Comet orbital parameters including Tisserand parameter for periodic and non-periodic comets relevant for current studies and observations. YYYY, MM, and DD.dddd: epoch for perturbed solution, q: perihelion distance, e: orbital eccentricity, ω: argument of perihelion, Ω: longitude of the ascending node, i: inclination, T: Tisserand parameter. H and y are absolute magnitude and slope parameter. Modified from www.cfa.harvard.edu/iau/Ephemerides/Comets/Soft00Cmt.txt

Comets	YYYY	MM	DD.dddd	Q [AU]	e	ϖ [°]	Ω [°]	i [°]	T	H	y
1P/Halley	1986	02	09.4589	0.58710	0.967277	111.8657	58.8601	162.2422	–0.069	4.0	18.0
2P/Encke	2007	04	19.3113	0.33927	0.847040	186.5233	334.5710	11.7542	4.834	11.0	16.0
4P/Faye	2006	11	15.6972	1.66347	0.567263	204.9326	199.2884	9.0413	3.238	4.5	10.0
6P/d'Arrest	2008	08	14.9576	1.35352	0.612774	178.1194	138.9356	19.5149	4.341	7.5	16.0
7P/Pons-Winnecke	2008	09	26.6316	1.25325	0.634923	172.3271	93.4225	22.3098	3.255	10.0	6.0
8P/Tuttle	2008	01	27.0002	1.02754	0.819736	207.5191	270.3443	54.9790	4.867	8.0	8.0
9P/Tempel	2011	01	12.1228	1.50862	0.517067	178.9266	68.9325	10.5266	2.889	5.5	10.0
10P/Tempel	2010	07	04.8493	1.42370	0.536198	195.5939	117.8351	12.0233	4.283	5.0	10.0
14P/Wolf	2009	02	27.2056	2.72415	0.358104	158.9747	202.1223	27.9413	0.533	5.5	12.0
15P/Finlay	2008	06	22.5668	0.96999	0.721431	347.4928	13.8077	6.8166	5.680	12.0	4.0
16P/Brooks	2008	04	12.6111	1.46659	0.562804	219.4796	159.3711	4.2585	3.017	7.5	10.0
17P/Holmes	2007	05	04.6635	2.05318	0.432774	24.3045	326.8545	19.1150	3.550	10.0	6.0
19P/Borrelly	2008	07	22.3392	1.35474	0.624512	353.3755	75.4432	30.3237	4.065	4.5	10.0
22P/Kopff	2009	05	25.4030	1.57762	0.544242	162.8146	120.8987	4.7239	3.180	3.0	10.4
24P/Schaumasse	2009	08	09.6414	1.21390	0.703538	58.0079	79.7179	11.7295	4.588	6.5	14.0
28P/Neujmin	2002	12	26.9690	1.55743	0.774834	347.6807	346.3108	14.3869	3.036	8.5	6.0
29P/Schwassmann-Wachmann	2004	06	29.3545	5.71764	0.044979	48.0970	312.6344	9.3947	–1.261	4.0	4.0
30P/Reinmuth	2010	04	19.6620	1.88422	0.500670	13.2288	119.7541	8.1225	2.372	9.5	6.0
31P/Schwassmann-Wachmann	2010	09	30.7823	3.42320	0.192110	18.1440	114.1877	4.5475	1.194	5.0	8.0
33P/Daniel	2008	07	20.3396	2.16968	0.461951	18.9713	66.5695	22.3745	1.221	10.0	12.0
43P/Wolf-Harrington	2010	06	30.8123	1.35307	0.596327	190.9356	250.4558	16.0758	2.916	8.0	6.0
44P/Reinmuth	2008	02	18.3327	2.10660	0.428428	58.0960	286.6008	5.9047	3.463	8.3	6.0
46P/Wirtanen	2008	02	02.4813	1.05726	0.658094	356.3319	82.1701	11.7395	5.198	9.0	6.0

Comets	YYYY	MM	DD.dddd	Q [AU]	e	ϖ [°]	Ω [°]	i [°]	T	H	y
47P/Ashbrook-Jackson	2009	01	31.9346	2.79910	0.319421	357.6764	356.9836	13.0515	3.041	1.0	11.2
49P/Arend-Rigaux	2011	10	18.3449	1.40670	0.603511	333.1531	118.9288	19.1183	4.370	11.3	4.4
50P/Arend	2007	11	01.1945	1.92394	0.529414	49.0371	355.3254	19.1574	3.602	9.5	6.0
51P/Harrington	2008	06	18.4092	1.68784	0.544318	269.1741	83.7763	5.4282	3.602	10.0	8.0
54P/de Vico-Swift-NEAT	2009	11	28.7923	2.17011	0.426916	2.0284	358.8964	6.0662	3.468	10.0	6.0
57P/du Toit-Neujmin-Delporte	2008	12	25.9975	1.72383	0.500265	115.3015	188.8334	2.8480	1.927	12.5	6.0
59P/Kearns-Kwee	2009	03	07.6462	2.35556	0.474993	127.5327	313.0363	9.3411	0.919	7.0	6.0
61P/Shajn-Schaldach	2008	09	06.0878	2.10801	0.426584	221.6274	163.1157	6.0090	3.503	6.0	10.0
64P/Swift-Gehrels	2009	06	14.2598	1.37698	0.689862	96.2913	300.7431	8.9518	2.955	8.5	12.0
65P/Gunn	2010	03	01.8606	2.44089	0.319654	196.5493	68.3675	10.3852	1.290	5.0	6.0
67P/Churyumov-Gerasimenko	2009	02	28.3606	1.24654	0.640176	12.6956	50.1978	7.0409	4.568	11.0	4.0
68P/Klemola	2009	01	20.9842	1.75902	0.640689	153.9800	175.3321	11.1436	2.977	10.0	4.0
74P/Smirnova-Chernykh	2009	07	30.7442	3.55750	0.147716	87.2996	77.1099	6.6478	2.964	5.0	6.0
77P/Longmore	2009	07	07.8153	2.31033	0.358286	196.6847	14.9185	24.3962	3.104	7.0	8.0
81P/Wild	2010	02	22.7608	1.59741	0.537402	41.8314	136.1003	3.2374	2.181	7.0	6.0
82P/Gehrels	2010	01	13.0724	3.63304	0.121727	226.4025	239.5187	1.1266	2.103	5.0	8.0
85P/Boethin	2008	12	16.3648	1.14747	0.775283	53.5814	343.4512	4.2171	4.070	6.5	8.0
86P/Wild	2008	05	19.8875	2.30077	0.366399	179.1225	72.5681	15.4420	0.955	11.0	6.0
88P/Howell	2009	10	12.4555	1.36375	0.561979	235.9378	56.7619	4.3816	3.386	11.0	6.0
89P/Russell	2009	08	17.1916	2.28002	0.399098	249.3204	42.3930	12.0327	3.259	11.5	6.0
93P/Lovas	2007	12	17.3437	1.70433	0.611883	74.6526	339.9199	12.2196	3.802	9.5	6.0
94P/Russell	2010	03	29.9348	2.23948	0.363015	92.9113	70.9210	6.1834	3.474	9.0	6.0
97P/Metcalf-Brewington	2011	08	23.5784	2.58101	0.459631	228.8719	185.3771	17.8698	2.648	5.5	6.0
99P/Kowal	2007	01	24.1723	4.72625	0.229838	173.8203	28.3028	4.3344	0.360	4.5	6.0
100P/Hartley	2009	12	06.1165	1.98226	0.418857	181.6965	37.8558	25.6525	3.515	9.0	8.0
110P/Hartley	2008	02	03.3255	2.48812	0.312487	167.7531	287.7439	11.6793	2.856	1.0	12.0

Comets	YYYY	MM	DD.dddd	Q [AU]	e	ϖ [°]	Ω [°]	i [°]	T	H	y
113P/Spitaler	2008	03	23.3867	2.12835	0.423157	49.8421	14.4660	5.7755	3.382	13.5	4.0
116P/Wild	2009	07	18.8682	2.17486	0.374774	173.5920	21.0371	3.6127	1.209	2.5	10.0
117P/Helin-Roman-Alu	2005	12	21.0427	3.04085	0.255626	222.9429	58.9428	8.7051	0.510	2.5	8.0
118P/Shoemaker-Levy	2010	01	02.2525	1.98488	0.427165	302.0916	151.8049	8.5084	1.826	12.0	4.0
119P/Parker-Hartley	2005	05	22.8617	3.04113	0.290309	181.1591	244.0770	5.1896	2.330	3.5	8.0
124P/Mrkos	2008	04	27.2348	1.46874	0.542393	181.3943	1.3441	31.3404	4.312	13.5	2.8
126P/IRAS	2010	02	22.8870	1.71351	0.696252	356.7494	357.7638	45.8274	2.690	6.0	8.0
127P/Holt-Olmstead	2009	10	21.3040	2.19480	0.363257	6.4967	13.7471	14.3132	2.062	11.0	6.0
128P/Shoemaker-Holt	2007	06	13.3857	3.06785	0.320087	210.4007	214.3946	4.3555	1.111	8.5	4.0
129P/Shoemaker-Levy	2005	09	13.1783	2.69325	0.280917	191.8046	300.9582	5.4667	2.821	11.0	4.0
136P/Mueller	2007	10	22.4643	2.96089	0.293353	224.9183	137.5533	9.4273	0.217	11.0	4.0
137P/Shoemaker-Levy	2009	05	13.5312	1.91527	0.574905	140.7831	233.1399	4.8535	2.753	11.0	4.0
139P/Vaisala-Oterma	2008	04	19.3546	3.40275	0.246828	165.5216	242.4512	2.3294	0.370	9.5	4.0
142P/Ge-Wang	2010	05	31.2358	2.48658	0.499016	175.8875	176.5508	12.3018	3.191	8.5	6.0
143P/Kowal-Mrkos	2009	06	12.1679	2.53819	0.410033	320.7470	245.3752	4.6897	1.940	13.5	2.0
144P/Kushida	2009	01	26.8620	1.43902	0.627754	216.0977	245.5607	4.1093	3.001	8.5	8.0
145P/Shoemaker-Levy	2009	03	26.5896	1.89140	0.542185	10.1288	26.9043	11.2990	2.952	13.5	4.0
147P/Kushida-Muramatsu	2008	09	22.9290	2.75641	0.275988	346.8722	93.7405	2.3672	0.794	14.0	4.0
148P/Anderson-LINEAR	2008	05	22.7375	1.70264	0.537868	6.6702	89.8020	3.6783	2.091	16.0	2.0
150P/LONEOS	2008	11	26.0004	1.76770	0.545854	245.6703	272.4293	18.5003	3.765	13.5	4.0
152P/Helin-Lawrence	2012	07	08.7895	3.11003	0.308492	163.9081	91.9618	9.8722	0.255	11.5	4.0
156P/Russell-LINEAR	2007	06	17.4026	1.59214	0.557832	357.6631	39.0288	20.7509	2.836	15.5	2.0
157P/Tritton	2010	02	20.2398	1.36383	0.601316	148.4907	300.1365	7.2838	4.117	10.0	4.0
158P/Kowal-LINEAR	2012	09	18.8746	4.58305	0.028954	231.8035	137.3088	7.9084	0.987	9.0	4.0
166P/NEAT	2002	05	12.8871	8.54590	0.381757	321.4598	64.4639	15.3749	–1.699	5.5	4.0
167P/CINEOS	2001	05	11.0442	11.8069	0.274059	344.5333	295.7664	19.0876	3.296	9.5	2.0
169P/NEAT	2009	11	30.3237	0.60751	0.766785	217.9702	176.2008	11.3001	8.364	16.0	2.0

Comets	YYYY	MM	DD.dddd	Q [AU]	e	ϖ [°]	Ω [°]	i [°]	T	H	y
172P/Yeung	2008	10	12.8451	2.24047	0.361814	179.0008	40.0883	11.5179	2.854	13.0	4.0
173P/Mueller	2008	05	18.1302	4.21431	0.260996	29.7886	100.5660	16.4948	–0.065	7.5	4.0
174P/Echeclus	2015	04	18.0978	5.83774	0.457674	162.4609	173.3629	4.3392	0.156	9.5	2.0
176P/LINEAR	2011	07	03.1902	2.57654	0.193113	35.9866	346.5218	0.2378	3.310	15.0	2.0
179P/Jedicke	2007	12	02.8687	4.08667	0.308340	295.4425	115.8485	19.8754	2.115	2.5	8.0
180P/NEAT	2008	05	26.7414	2.46876	0.357485	94.9254	84.7513	16.9138	1.557	11.0	4.0
183P/Korlevic-Juric	2008	05	08.7657	3.89391	0.135463	161.6319	5.8424	18.7337	3.021	12.5	2.0
186P/Garradd	2008	03	23.3658	4.26406	0.119717	279.1100	327.8136	28.8535	–0.362	7.5	4.0
187P/LINEAR	2008	10	06.6783	3.69315	0.170670	132.0082	112.0014	13.7325	2.021	9.0	4.0
188P/LINEAR-Mueller	2007	12	16.2089	2.55210	0.416222	26.4576	359.1388	10.5456	1.394	11.5	4.0
191P/McNaught	2007	09	13.1617	2.04763	0.420348	274.1713	106.5264	8.7611	1.527	13.0	4.0
195P/Hill	2009	01	21.1344	4.43858	0.314862	249.6219	243.2517	36.3623	1.541	8.5	4.0
196P/Tichy	2008	02	07.1756	2.13778	0.434032	11.7251	24.3335	19.3775	3.357	13.5	4.0
197P/LINEAR	2008	05	19.0057	1.06040	0.629921	188.7878	66.3858	25.5545	5.368	16.5	2.0
199P/Shoemaker	2009	04	09.8986	2.93531	0.507536	191.9396	92.9480	24.7661	2.936	10.0	4.0
200P/Larsen	2008	08	25.2370	3.27203	0.333288	133.7395	234.8172	12.1211	2.905	9.0	4.0
201P/LONEOS	2008	08	04.7584	1.34500	0.611677	24.9633	35.2995	7.0324	4.318	14.0	4.0
202P/Scotti	2009	02	07.0219	2.52705	0.330740	255.5572	194.5826	2.1849	1.205	13.5	4.0
203P/Korlevic	2010	02	08.2319	3.18242	0.314639	154.5436	290.5611	2.9760	0.077	14.5	2.0
204P/LINEAR-NEAT	2008	12	09.2711	1.94024	0.470561	355.0388	109.1065	6.5812	3.628	14.0	4.0
205P/Giacobini	2008	09	10.0558	1.52644	0.568719	154.2271	179.6311	15.3038	2.440	13.0	4.0
207P/NEAT	2008	11	06.2547	0.94415	0.757147	271.1732	200.6739	10.1500	4.871	16.0	4.0
208P/McMillan	2008	05	13.3110	2.52505	0.374412	310.5032	36.4171	4.4134	1.592	12.5	4.0
209P/LINEAR	2009	04	15.9729	0.91370	0.688980	149.7234	66.4549	19.1480	6.065	17.0	2.0
210P/Christensen	2008	12	19.9718	0.53491	0.831644	345.7777	93.8869	10.2154	9.092	13.5	4.0
211P/Hill	2009	05	07.8248	2.36203	0.337560	4.4118	117.2959	18.8724	3.410	12.5	4.0

Comets	YYYY	MM	DD.dddd	Q [AU]	e	ϖ [°]	Ω [°]	i [°]	T	H	y
212P/NEAT	2008	12	03.2697	1.65447	0.578876	15.0488	98.9290	22.3979	2.161	17.0	2.0
213P/Van Ness	2011	06	15.7382	2.12476	0.379641	3.1425	312.6973	10.2418	1.528	10.5	4.0
214P/LINEAR	2009	01	05.6163	1.84373	0.488740	190.2693	348.2590	15.2132	1.779	13.0	4.0
215P/NEAT	2010	06	07.3698	3.21463	0.200731	222.3052	75.4472	12.7900	3.087	11.0	4.0
C/1995 O1 (Hale-Bopp)	1997	03	31.0395	0.91576	0.994964	130.6418	282.9359	89.2217	5.486	−2.0	4.0
P/1998 QP54 (LONEOS-Tucker)	2007	05	12.2904	1.87942	0.552375	30.3480	341.7955	17.7148	3.092	15.0	2.0
P/1998 U4 (Spahr)	2012	04	24.4836	3.85427	0.309940	251.7638	181.6010	31.5065	2.960	8.0	4.0
P/1998 VS24 (LINEAR)	2008	05	24.7069	3.42256	0.242438	244.3849	159.1784	5.0262	1.956	13.0	2.0
P/1999 XB69 (LINEAR)	2009	07	25.9281	1.65211	0.630655	220.3337	256.0529	11.3063	3.299	17.5	2.0
P/1999 XN120 (Catalina)	2008	11	12.5113	3.30408	0.210838	161.6110	285.4487	5.0263	2.004	13.5	2.0
P/2000 Y3 (Scotti)	2011	12	26.2613	3.97492	0.202027	88.3103	354.4006	2.2619	0.145	9.0	4.0
P/2001 CV8 (LINEAR)	2008	10	11.3415	2.15996	0.444133	151.6005	359.8919	9.0358	1.225	9.0	4.0
P/2001 MD7 (LINEAR)	2009	09	08.9792	1.22338	0.689638	246.7813	125.6229	12.8817	4.768	12.0	4.0
P/2001 YX127 (LINEAR)	2011	08	26.0287	3.42968	0.176271	115.0431	31.0718	7.9171	1.355	14.5	2.0
P/2002 JN16 (LINEAR)	2009	01	25.0993	1.78370	0.487252	39.6995	230.0342	11.4189	3.232	14.5	4.0
P/2002 LZ11 (LINEAR)	2010	03	06.5856	2.36378	0.352625	107.8521	231.1001	11.5240	2.764	11.0	4.0
P/2002 Q1 (Van Ness)	2009	03	20.9526	1.55117	0.564027	185.0191	173.9989	36.2774	3.360	13.0	4.0
P/2002 S1 (Skiff)	2010	08	15.7053	2.41441	0.417420	38.1832	346.8741	27.0413	1.652	11.0	4.0
C/2002 VQ94 (LINEAR)	2006	02	06.6280	6.79806	0.964240	100.0739	34.9971	70.5458	0.822	9.5	2.0
P/2003 A1 (LINEAR)	2009	06	16.0078	1.91626	0.499959	340.2462	54.0811	44.3324	3.617	13.5	4.0
P/2003 CP7 (LINEAR-NEAT)	2011	05	18.2863	3.02968	0.246366	42.7503	133.0997	12.3291	3.117	14.5	2.0
P/2003 H4 (LINEAR)	2009	06	22.3878	1.70150	0.490365	10.5887	226.7468	18.1509	3.717	16.0	4.0
P/2003 O3 (LINEAR)	2009	01	30.0140	1.24673	0.598534	0.6922	341.4904	8.3653	3.619	18.0	4.0
C/2003 WT42 (LINEAR)	2006	04	10.2392	5.19092	0.999995	92.4639	48.4388	31.4243	0.970	11.5	2.0
P/2004 A1 (LONEOS)	2004	09	06.5657	5.48879	0.310552	21.9953	124.9768	10.5509	0.054	6.5	4.0
C/2004 D1 (NEAT)	2006	02	10.3179	4.97537	0.999006	75.5451	62.2441	45.5488	1.005	11.5	2.0

Comets	YYYY	MM	DD.dddd	Q [AU]	e	ϖ [°]	Ω [°]	i [°]	T	H	y
P/2004 F3 (NEAT)	2005	01	05.1336	2.86999	0.286234	176.4231	78.8214	15.985	0.345	9.0	4.0
P/2004 FY140 (LINEAR)	2004	08	03.4498	4.11096	0.167025	239.6618	327.1830	2.1268	0.273	12.5	2.0
P/2005 L1 (McNaught)	2005	12	14.4885	3.14701	0.209017	149.8632	138.3064	7.7356	1.772	9.5	4.0
C/2005 L3 (McNaught)	2008	01	16.4352	5.59380	0.999768	47.1431	288.7407	139.450	0.910	4.0	4.0
P/2005 RV25 (LONEOS-Christensen)	2006	11	05.4639	3.60516	0.166205	191.4092	246.9033	9.8835	–0.115	9.5	4.0
P/2005 S2 (Skiff)	2006	06	27.9379	6.39701	0.197944	229.7722	161.2220	3.1405	–1.436	7.5	4.0
C/2005 S4 (McNaught)	2007	07	19.3179	5.85150	0.998670	31.5247	318.2891	107.960	0.901	5.0	4.0
P/2005 SB216 (LONEOS)	2007	02	10.8989	3.81646	0.463198	83.5061	1.6746	24.1084	2.115	12.0	2.0
C/2005 YW (LINEAR)	2006	12	06.6725	1.99972	0.987926	234.8270	302.0415	40.8288	2.304	10.0	4.0
P/2006 F1 (Kowalski)	2008	02	19.8337	4.11959	0.119527	186.8718	124.7624	21.2754	–0.146	8.0	4.0
C/2006 K4 (NEAT)	2007	11	29.4497	3.18902	0.998079	233.6402	116.6035	111.345	1.550	6.0	4.0
C/2006 P1 (McNaught)	2007	01	12.5909	0.17109	0.999942	155.9911	267.4092	77.8424	29.222	6.0	4.0
C/2006 Q1 (McNaught)	2008	07	03.8594	2.76367	0.999682	344.3821	199.5469	59.0495	1.779	5.0	4.0
P/2006 R2 (Christensen)	2006	06	15.9829	3.04011	0.271323	189.0242	139.1297	16.3171	0.414	11.0	4.0
C/2006 S3 (LONEOS)	2012	04	17.3515	5.13989	0.999573	140.0253	38.3231	166.028	0.920	2.0	4.0
C/2006 S5 (Hill)	2007	12	09.6700	2.62987	0.972713	182.0871	281.5577	10.1312	1.645	8.0	4.0
C/2006 U6 (Spacewatch)	2008	06	05.4956	2.49836	0.998757	276.6045	180.1823	84.8807	1.931	8.0	4.0
C/2006 V1 (Catalina)	2007	11	26.5796	2.67391	0.990562	253.4765	335.6326	31.1716	2.064	8.0	4.0
C/2006 W3 (Christensen)	2009	07	06.6378	3.12634	0.999782	133.5099	113.5707	127.075	1.605	5.0	4.0
C/2007 B2 (Skiff)	2008	08	20.9030	2.97491	0.995838	206.0121	14.8692	27.4959	1.581	6.0	4.0
P/2007 C2 (Catalina)	2007	09	04.2929	3.77858	0.462212	179.4127	276.1100	8.6736	0.196	10.0	4.0
C/2007 D1 (LINEAR)	2007	06	17.9972	8.79237	0.998115	340.1052	171.0873	41.5298	0.443	3.5	4.0
C/2007 D3 (LINEAR)	2007	05	27.5460	5.20793	0.992286	309.0691	148.4264	45.9277	0.867	7.5	4.0
P/2007 H1 (McNaught)	2007	08	17.8241	2.28132	0.378351	202.6697	144.3666	11.8743	3.155	10.0	4.0
C/2007 K1 (Lemmon)	2007	05	09.4553	9.24063	0.980070	52.0531	294.6533	108.429	0.517	6.0	4.0
C/2007 M1 (McNaught)	2008	08	11.7961	7.47494	0.995217	52.6403	326.8090	139.721	0.688	6.0	4.0

Comets	YYYY	MM	DD.dddd	Q [AU]	e	ϖ [°]	Ω [°]	i [°]	T	H	y
C/2007 M2 (Catalina)	2008	12	08.5909	3.54090	0.999077	220.6739	357.2846	80.9522	1.466	8.0	4.0
C/2007 M3 (LINEAR)	2007	09	04.3461	3.46902	0.979213	125.7387	41.6689	161.743	1.425	9.5	4.0
C/2007 N3 (Lulin)	2009	01	10.6395	1.21227	0.999991	136.8656	338.5391	178.374	4.121	6.5	4.0
P/2007 R1 (Larson)	2007	08	23.7997	4.35242	0.278173	175.1484	181.6574	7.8753	1.111	8.0	4.0
P/2007 S1 (Zhao)	2007	12	06.7033	2.49438	0.343312	245.3891	141.6164	5.9725	3.268	13.0	4.0
C/2007 S2 (Lemmon)	2008	09	14.5951	5.55796	0.556827	210.4439	296.2499	16.8615	0.190	6.5	4.0
C/2007 T5 (Gibbs)	2008	05	24.0866	4.04923	0.913014	34.3931	109.8413	45.6144	1.190	8.0	4.0
P/2007 V1 (Larson)	2007	12	08.4574	2.67630	0.461373	51.4428	8.1728	10.7897	1.603	12.0	4.0
P/2007 VQ11 (Catalina)	2008	02	13.5648	2.69337	0.502201	277.6597	164.0500	12.3263	3.089	12.0	4.0
C/2007 VO53 (Spacewatch)	2010	04	26.3622	4.84282	0.999819	75.0143	59.7508	87.0049	1.054	7.0	4.0
C/2007 W1 (Boattini)	2008	06	24.8774	0.84964	0.999970	306.5407	334.5207	9.8891	5.879	9.5	4.0
C/2007 Y2 (McNaught)	2008	04	08.4294	4.20903	0.995941	257.6941	303.4632	98.5029	1.115	9.0	4.0
C/2008 C1 (Chen-Gao)	2008	04	16.8380	1.26234	0.999907	180.9219	307.7822	61.7852	3.968	10.0	4.0
C/2008 E1 (Catalina)	2008	08	11.8316	4.82895	0.548176	269.9867	189.0234	35.0376	–0.423	7.0	4.0
C/2008 E3 (Garradd)	2008	08	02.2971	5.53096	0.997634	218.1015	105.6737	105.076	0.880	6.0	4.0
C/2008 G1 (Gibbs)	2009	01	12.1249	3.98899	0.988850	63.7326	215.9135	72.8480	1.033	9.5	4.0
C/2008 H1 (LINEAR)	2008	03	16.3883	2.76003	0.945675	96.0369	34.6356	75.4932	2.292	10.5	4.0
C/2008 J1 (Boattini)	2008	07	13.2692	1.72434	0.989673	68.1270	273.4202	61.7796	2.983	10.0	4.0
P/2008 J2 (Beshore)	2008	03	20.9627	2.40995	0.308370	131.8234	98.2973	10.2673	1.196	9.0	4.0
P/2008 J3 (McNaught)	2009	03	10.6932	2.28719	0.412474	4.3957	9.8573	25.3978	3.375	12.0	4.0
P/2008 L2 (Hill)	2008	08	18.6147	2.31741	0.613838	141.3214	217.9843	25.8603	2.960	12.5	4.0
C/2008 N1 (Holmes)	2009	09	25.8657	2.78386	0.997034	100.7973	357.4642	115.512	1.710	9.0	4.0
P/2008 O2 (McNaught)	2009	04	21.1067	3.80374	0.154393	27.4010	325.8579	9.5167	–0.402	9.0	4.0
P/2008 O3 (Boattini)	2008	06	03.1295	2.49752	0.695305	340.9991	47.5730	32.2692	2.670	13.0	4.0
C/2008 Q1 (Maticic)	2008	12	30.1093	2.95923	0.995071	104.4745	9.3084	118.627	1.801	10.0	4.0
P/2008 Q2 (Ory)	2008	10	19.0057	1.38234	0.573647	329.5862	60.7087	2.7553	2.819	16.5	4.0
C/2008 Q3 (Garradd)	2009	06	23.1361	1.79600	0.999030	340.9155	219.7112	140.706	2.742	10.0	4.0

Comets	YYYY	MM	DD.dddd	Q [AU]	e	ϖ [°]	Ω [°]	i [°]	T	H	y
P/2008 QP20 (LINEAR-Hill)	2008	11	02.7128	1.72309	0.506310	72.0504	325.1485	7.7493	3.008	15.5	4.0
C/2008 R3 (LINEAR)	2008	11	22.4877	1.90892	0.895944	84.1555	270.5582	43.2377	3.023	13.0	4.0
P/2008 S1 (Catalina-McNaught)	2008	10	01.8295	1.19022	0.666330	203.6318	111.3909	15.1013	3.603	15.0	4.0
P/2008 T1 (Boattini)	2008	02	26.7412	3.04343	0.280983	35.9841	291.7259	2.0829	0.909	11.0	4.0
P/2008 T4 (Hill)	2008	12	23.9088	2.51187	0.435111	1.2452	44.6833	6.3266	3.266	13.5	4.0
P/2008 WZ96 (LINEAR)	2009	01	23.9350	1.64604	0.509106	337.6342	59.1164	6.9575	3.809	13.5	4.0
C/2008 X3 (LINEAR)	2008	10	10.5813	1.90202	0.956445	140.7970	337.7503	66.473	2.313	13.0	4.0
P/2008 Y1 (Boattini)	2009	02	25.1350	1.27141	0.733912	162.4022	259.7291	8.8044	3.375	15.0	4.0
P/2008 Y2 (Gibbs)	2009	01	22.4120	1.63841	0.543575	162.3438	330.8931	7.2751	3.577	16.0	4.0
P/2008 Y3 (McNaught)	2009	01	11.9679	4.43422	0.447555	238.2773	262.9372	38.8144	1.869	8.5	4.0
P/2009 B1 (Boattini)	2009	02	06.2096	2.42665	0.637248	128.5988	297.4354	22.2292	1.017	13.0	4.0
C/2009 B2 (LINEAR)	2009	03	07.7050	2.32848	0.951370	192.6290	18.8320	156.888	2.560	12.5	4.0
P/2009 D1 (LINEAR)	2008	10	10.9767	2.15988	0.444137	151.5970	359.8931	9.0351	1.226	9.0	4.0

Nomenclature of comets

In 1994, IAU introduced a new comet-designation scheme that more closely resembles the minor-planet designation scheme [95M1, 95M2]. In the new scheme comets are assigned a year-letter-number designation specifying the year of discovery, followed by an upper-case letter identifying the half-month of discovery and a consecutive number indicating the order of discovery announcement in that half month (the year and half-month/sequence-number being separated by a single space).

This designation is preceded by a "P/" for periodic comets with periods < 200 years or a "C/" for a single-apparition comet (P > 200 years). If the orbit cannot be computed the prefix "X/" is used and comets that have disappeared receive the prefix "D/". If a comet splits in two or more fragments, the components are distinguished by appending -A, -B, -C,… The tradition of naming a comet after its discoverer has been maintained, whereby the name of the discoverer is now given in parenthesis after the official designation. Conversion from old designation to the new ones can be obtained at: www.cfa.harvard.edu/iau/CometDes.html.

Sun-grazing comets

These Comets are passing so close to the Sun that their perihelion distance is measured in solar radii rather than Astronomical Units. The first Sun-grazing comet with a computed orbit was the great comet of 1860 - 1861, which had a perihelion distance of only 0.3 solar radii above the photosphere. Solar coronographs implemented on space missions such as "Solwind", "Solar Maximum Mission" (SMM) and the "Solar and Heliospheric Observatory" (SOHO), have discovered more than 1600 Sun-grazing comets. Many of them belong to the Kreutz group, which is presumed to have been produced by the fragmentation of a very large comet several centuries ago [05S, 07S2]. A review on Sun-grazing comets is given by [05M2]. Updated information on the last discoveries can be found online at Sungrazer.nrl.navy.mil.

4.3.4.2 Photometry and polarimetry

Photometry

Brightness variation of comets:

Intrinsic brightness J_0 at r = 1 AU and Δ = 1 AU is related to the observed brightness J by the equation $J = J_0 \Delta^{-2} r^{-n}$ (Δ = geocentric distance, r = heliocentric distance, both in [AU] where n is derived for each comet from observation, with mean values ranging from 2 to 8. However, the value of n is not constant for a given comet, but depends on its activity variation with heliocentric distance, sometimes changing abruptly.

The predicted apparent magnitude m is calculated as $m = H_y + 5 \log \Delta + y \log r$, with $y = 2.5\, n$. The mean value of y is often assumed as 10 and H_y is assumed as a constant depending only on y and commonly referred to as the "absolute magnitude" (for $\Delta = r = 1$ AU). In reality, however, the value of y is ranging from 5 to 28!

Visual magnitude estimations are strongly depending on the observational techniques and physical factors of the comet such as the gas (particularly C_2) to dust ratio. Nowadays they are used as a tool for observational planning and for light curves provided by amateur observers [91L].

Values for the activity of a comet are usually provided as $Af\rho$ (dust activity) and Q (gas production rate). $Af\rho$ is the product of Bond Albedo (A), filling factor of grains in the aperture (f), and aperture radius (ρ). It can be derived by aperture photometry or long-slit spectroscopy and is, for steady-state comets, not dependent on aperture size. $Af\rho$ is approximately proportional to the dust production rate [84A1]. The gas production rate Q (in molecules s^{-1}) can be derived by spectroscopy or narrow-band gas emission filters using photolytic coma models. A recent review and a discussion of limitations are given in [06S2].

Photometric systems

The standard broad-band filters, designed for stellar photometry, are not suited for cometary work since they do not isolate the various coma emitters. For modern photometric measurements to have substance, the bandpasses must be selected to record the emission of a well-identified (or dominant) emitter.

The International Halley Watch, IHW photometric system was developed for the 1986 apparition of comet 1P/Halley and introduced in the photoelectric photometry of comets. It consisted of six interference filters for molecular bands and three for the continuum [84A2, 90O]. Later, two new filters sets, called the Hale-Bopp and the ESA set, were defined in a coordinated effort by the US and Europe [96S, 00F]. Both include additional filters and revised bandpass for some filters.

From pure molecular emission flux density F_m [J m^{-2} s^{-1}] measured in the column of coma defined by the diaphragm of the photometer or the pixel size of a CCD detector the total number of molecules can be derived as

$$N_m = 4\pi F_m \Delta^2 r^2 / g \tag{2}$$

where the geocentric distance Δ is given in [m] and the heliocentric distance r in [AU]. The fluorescence efficiency g for typical molecular emissions at r = 1 AU is of the order of 10^{-19} to about 10^{-22} J s^{-1} molecule^{-1}. In the literature values are used for the g-factor of the same transition that show discrepancies of up to a factor of 10 [06S2].

Infrared photometry

At wavelengths from 1 to 2.5 μm the standard infrared photometric bandpasses J, H, K are used to study the dust component of the coma and derive *Afρ* values in the near-IR, where only few weak gas emission bands are present.

Beyond 2.5 μm thermal emission from the dust becomes the dominant. The region is probed by standard M, N Q filters, as well as narrow-band filters centred on the silicate emission feature at 10 μm. A recent review can be found in [04K].

Table 2. Narrow-Band filters used for comet research. (FWHM = full width half maximum)

Spectral feature	IHW [84A2, 90O]		Hale Bopp [00F]		ESA [96S]	
	Central wavelength λ [nm]	FWHM [nm]	Central wavelength λ [nm]	FWHM [nm]	Central wavelength λ [nm]	FWHM [nm]
OH(0-0)	308.5	8.0	309.0	6.2	308.5	7.5
NH(0-0)	-	-	336.2	5.8	-	-
UV Cont.	365.0	8.0	344.8	8.4	-	-
CN(Δv = 0)	387.1	5.0	387.0	6.2	387.0	5.0
C3	406.0	7.0	406.2	6.2	406.0	7.0
CO^+ (2-0)	426.0	7.0	426.6	6.4	-	-
Blue Cont.	484.5	6.5	445.0	6.7	443.0	4.0
C_2 (Δv = 0)	514.0	9.0	514.1	11.8	512.5	12.5
Green Cont.	-	-	526.0	5.6	-	-
NH_2 (0,2,0)	-	-	663.0	6.0	663.0	6.0
Red Cont.	684.0	9.0	712.8	5.8	684.0	9.0
H_2O^+ (0,6,0)	700.0	8.0	702.0	17.0	-	-

Table 3. Visual brightness, m_v, CN production rate, and $Af\rho$ for recent bright comets. Note, m_v provided by amateur observations.

Comet	Date	r [AU]	Δ [AU]	m_v	Q_{CN} [mol s^{-1}]	$Af\rho$ [cm]	Ref.
1P/Halley	30.12.1985	1.029	1.131	4.3	8.5×10^{26}	3600	[98S1]
C/1996 B2 Hyakutake	25.03.1996	1.045	0.102	0 - 2	3.3×10^{26}	5750	[02S2]
46P/Wirtanen	15.03.1997	1.070	1.536	10	7.9×10^{23}	120	[98S3]
C/1999 S4 (LINEAR)	12.06.2000	1.132	1.645	10	3.1×10^{25}	575	[01F]
19P/Borrelly	24.12.1987	1.359	1.488	-	5.0×10^{25}	407	[03S]
81P/Wild 2	01.05.1987	1.584	1.150	-	1.7×10^{25}	295	[05F]
9P/Tempel 1	03.07.2005	1.506	0.889	10	8.3×10^{24}	105	[07S1]
67P/Churyumov-Gerasimenko	21.01.1996	1.301	1.095	11	6.3×10^{24}	89	[06S1]
96P/ Machholz	12.05.2007	1.074	0.657	12	6.0×10^{22}	28	[08S1]
C/1994 O1 (Hale-Bopp)	15.02.1997	1.207	1.730	0-1	1×10^{28}	400000	[97S]

Polarimetric observations

As solar radiation is scattered by coma grains linear polarization occurs. The scattered light is characterized by Stokes parameters [07L]. As the preferred direction of the scattering angle lies in the plane of Sun-comet-observer, the linear degree of polarisation P can more simply be described by the components parallel ($I_{\parallel}$) and perpendicular ($I_{\perp}$) to this plane. By convention P is given as:

$$P = (I_{\perp} - I_{\parallel})/(I_{\perp} + I_{\parallel}) \text{ with the total intensity } I = (I_{\perp} + I_{\parallel}). \quad (3)$$

P changes with the scattering angle ($\angle$ Sun-comet-observer) that is equivalent to the phase angle α. (The measured phase dependence is similar to that of asteroids [02M], which is unusual, because for a solid body multiple scattering occurs whereas for the optically thin coma single scattering is expected.) Back scattering ($P \approx 0$) occurs at $\alpha = 0°$. With increasing phase angle, P decreases to negative values ($I_{\parallel} < I_{\perp}$) reaching a minimum of a few percent at $\alpha \approx 10°$ and increases again crossing zero polarization at $\sim 20°$ and reaching a maximum (15% to 30%) at $\alpha = 90°$. No differences exist between comets in region of negative polarization ($\alpha < 20°$). For $\alpha > 20°$ values of P vary with comet. Two classes have been identified. Comets with low maximum polarization degree also have a low dust to gas ratio; comets with high maximum polarization are very dusty. P may be correlated with strength of silicate band at 10 μm. Discussions see in [96L1, 99K, 05J].

Very few polarimetric measurements exist of comet nuclei indicating a phase dependence different from that of the coma and asteroids and more similar to trans-Neptunian-objects [08B1, 08B2].

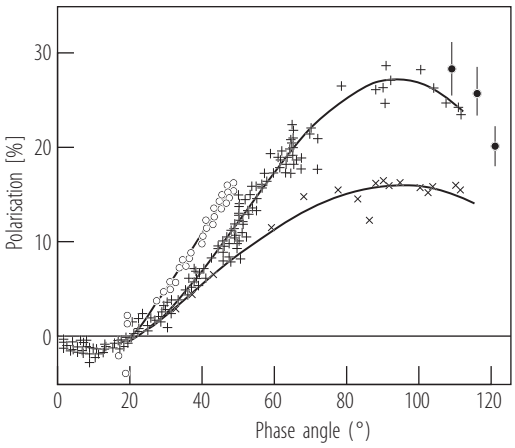

Fig. 3. Coma polarization (measured in narrow band red filter) as a function of phase angle: (×) comets with low maximum in polarization, (+) comets with higher maximum, (○) comet C/1995 O1 (Hale-Bopp) and (●) comet C/1999 S4 (LINEAR) [from 04K].

4.3.4.3 Multi-wavelength spectroscopic observations

In an active comet the nucleus is hidden in the coma. Remotely, comet nuclei can only be observed at large heliocentric distance, where they have been detected spectroscopically at optical and near-IR wavelengths [07C]. The coma (constituting of solid state and gaseous components) is observable from radio wavelengths to X-rays.

Emission of gas coma

It is mainly due to resonant scattering of solar radiation. A gas molecule (or ion) is excited by absorbing solar radiation corresponding to the excitation energy, and decays spontaneously by emitting the radiation at the same wavelength over 4π. Electronic, ro-vibrational, and for polar species, rotational transitions are possible. Electronic transitions produce radiation in the UV, and visible spectral range. The strength of emission depends on fluorescence efficiency. Ro-vibrational transitions radiate in the IR. Rotational transitions radiate in the radio domain.

In few cases prompt-emission occurs. The dissociation of parent molecules produces daughter products (see 4.3.4.6). If daughter species is produced in an excited state its successive radiative decay produces prompt emission which allows tracing the parent molecule(s).

Emission of dust coma

For wavelength shorter than about 3 μm continuum radiation is produced by Sunlight scattered by the dust particles in coma (and tail). Thermal emission and solid state emission bands are present at longer IR wavelengths.

X-ray observations

Soft X-ray emission (E < 1 keV) from comets was discovered with ROSAT in 1996. Observed characteristics are very specific in spatial morphology, total X-ray luminosity, temporal variation, and energy spectrum. Emission is caused by charge exchange between solar wind ions and neutrals in the coma (mainly water and its dissociation products). This has been proven by the observation of X-ray emission lines expected from the de-excitation of highly charged states of heavy ions (mainly C,N,O) with Chandra and XMM-Newton. Reviews in [04L2, 07B1].

UV observations

Most observations have been obtained with the International Ultraviolet Explorer, IUE, (1978 - 1996), and the Hubble Space Telescope, HST (1990-present). Observations with satellites and sounding rockets (pre-IUE) are summarized in [82F]. FUSE observatory (1999-present) provides access to spectral region between 900 and 1200 Å. Spectra appear with very low continuum and many emission lines, mostly of CO. For recent review see [04F1].

Optical observations

Spectra are composed of continuum superimposed by emissions. The continuum is mainly produced from Sunlight scattered at dust particles in coma and tail. Only a very small fraction is due to solar radiation reflected by the nucleus. The energy distribution in the continuum is determined by size and optical characteristics (index of refraction) of small particles and the scattered light is often slightly redder than Sunlight. Emissions (molecular bands or atomic lines) are due to neutral radicals or atoms and ions. At small heliocentric distances metallic lines are often observed. Due to the heliocentric component of the comet's motion the Fraunhofer lines in the solar spectrum are Doppler shifted relative to the comet: influence on the vibration-rotation line intensities in the molecular bands (Swings-effect). A similar secondary effect (Greenstein effect) is due to the internal motion (expansion) in the coma.

High resolution spectra of molecular bands permit observation of the individual transitions occurring from different vibrational states, hence determining the relative population in these states. This allows verification of whether the population is in equilibrium, determination of excitation temperature and detection of molecular isomers. Isotopic ratios are available of D/H, $^{12}C/^{13}C$, $^{14}N/^{15}N$, $^{16}O/^{18}O$, and $^{32}S/^{34}S$ [04B3, 09M].

Infrared observations

The 1 - 2.5 μm region is dominated by scattering of the solar radiation at cometary grains. Few faint emissions of CN are also present. Beyond 2.5 - 3 μm the thermal emission of the grains begins to dominate reaching an equilibrium temperature when the absorbed radiation (mainly from the visible) is equal to the emitted radiation in the infrared.

For a black body the equilibrium temperature depends only on the heliocentric distance. Often the grains are at equilibrium temperature, but for small grains the emission coefficient is very low and the grains reach a temperature higher than that of equilibrium.

Most of the ro-vibrational transitions of complex organic molecules are in the region around 3.5 μm [04B3].

Radio observations

Rotational transitions of parent molecules are detected at radio wavelengths in the mm and in the sub-mm regions. Most molecules detected to date were found in comet C/1995 O1 (Hale-Bopp). Their abundance was monitored as a function of pre- and post-perhelion orbit, [97B1, 02B1]. Observations of other comets are given in [02B2], a review was written by [04B3]. Sub-mm observations performed with the Odin satellite in [07B2].

The OH radical detected in the cm region [02C] was for long time the only way to derive water production rates in comets.

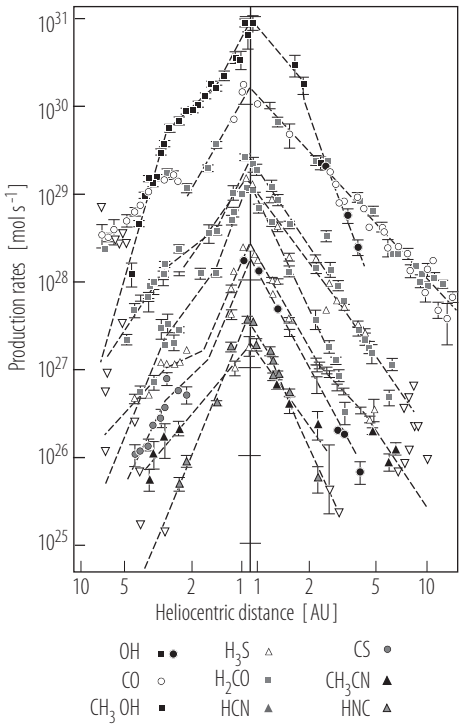

Fig. 4. Gas production rates in comet C/1996 O1 (Hale-Bopp) from radio observations. Inverted triangles indicate upper limits in case of non-detection. From [02B1].

Table 4. Principal emission bands [04F1]

Species	Transition	System	λ [nm]
OH	$A^2\Sigma^+ - X^2\Pi_I$ (0,0)		308.5
CN	$B^2\Sigma^+ - X^2\Sigma^+$ (0,0)	Violet	388.3
	$A^2\Pi - X^2\Sigma^+$ (2,0)	Red	787.3
C_2	$D^3\Pi_g - a^3\Pi_u$ (0,0)	Swan	516.5
	$A^1\Pi_u - X^1\Sigma_g^+$ (3,0)	Phillips	771.5
	$D^1\Sigma_u^+ - X^1\Sigma_g^+$ (0,0)	Mulliken	231.3
C_3	$\tilde{A}^1\Pi_u - X^1\Sigma_g^+$	Comet Head Group	344.0 - 410.0
CH	$A^2\Delta - X^2\Pi$ (0,0)		431.4
	$B^2\Sigma^- - X^2\Pi$ (0,0)		387.1, 388.9
CS	$A^1\Pi - X^1\Sigma^+$ (0,0)		257.6
NH	$A^3\Pi_i - X^3\Sigma^-$ (0,0)		336.0
NH_2	$\tilde{A}^2A_1 - \sim X^2B_1$		450.0 - 735.0
OI (^{1}D)*	$^1D - ^3P$		630.0, 636.4
OI (^{1}S)*	$^1S - ^1D$		557.7
CI (^{1}D)*	$^1D - ^3P$		982.3, 984.9
CO^+	$B^2\Sigma^+ - X^2\Sigma^+$ (0,0)	First Negative	219.0
	$A^2\Pi - X^2\Sigma^+$ (2,0)	Comet Tail	427.3
CO_2^+	$\sim B^2\Sigma_u - \sim X^2\Pi_g$		288.3, 289.6
	$\tilde{A}^2\Pi_u - \sim X^2\Pi_g$	Fox-Duffendack-Barker	280.0 - 500.0
CH^+	$A^1\Pi - X^1\Sigma^+$ (0,0)	Douglas-Herzberg	422.5, 423.7
OH^+	$A^3\Pi - X^3\Sigma^-$ (0,0)		356.5
H_2O^+	$\tilde{A}^2A_1 - \sim X^2B_1$		427.0 - 754.0
N_2^+	$B^2\Sigma^+ - X^2\Sigma^+$ (0,0)	First Negative	391.4

*Prompt emission

Table 5. Production rates relative to water in bright comets at r = 1 AU [04B3].

Molecule	1P/Halley	C/1995 O1 (Hale-Bopp)	C/1996 B2 (Hyakutake)	C/1999 H1 (Lee)	C/1999 S4 (LINEAR)	153P/2002 C1 (Ikeya-Zhang)
H_2O	100	100	100	100	100	100
CO	3.5*, 11	12*, 23	14*,19 - 30	1.8 - 4	≤ 0.4, 0.9	2,4 - 5
CO_2	3 - 4	6	-	-	-	-
CH_4	< 0.8	1.5	0.8	0.8	0.14	0.5
C_2H_2	0.3	0.1 - 0.3	0.2 - 0.5	0.27	< 0.12	0.18
C_2H_6	0.4	0.6	0.6	0.67	0.11	0.62
CH_3OH	1.8	2.4	2	2.1	< 0.15	2.5
H_2CO	4	1.1	1	1.3	0.6	0.4
HCOOH	-	0.09	-	-	-	< 0.1
$HCOOCH_3$	-	0.08	-	-	-	-
CH_3CHO	-	0.02	-	-	-	-
NH_2CHO	-	0.015	-	-	-	-
NH_3	1.5	0.7	0.5	-	-	< 0.2
HCN	0.1	0.25	0.1	0.1	0.1	0.1 - 0.2
HNCO	-	0.10	0.07	-	-	0.04
HNC	-	0.04	0.01	0.01	0.02	0.005
CH_3CN	-	0.02	0.01	-	-	0.01
HC_3N	-	0.02	-	-	-	< 0.01
H_2S	0.4	1.5	0.8	< 0.9	0.3	0.8
OCS	-	0.4	0.1	-	-	< 0.2
SO_2	-	0.2	-	-	-	-
CS_2	0.2	0.2	0.1	0.08	0.12	0.06 - 0.1
H_2CS	-	0.05	-	-	-	-
NS	-	≥ 0.02	-	-	-	-
S_2	-	-	0.005	0.002	0.0012	0.004

* Production from the nucleus

Table 6. Molecular upper limits (3σ) in C/1995 O1 (Hale-Bopp) from radio observations [04C5].

Molecule	[X]/[H_2O]
H_2O	100
$(H_2O)_2$	< 0.5
H_2O_2	< 0.03
CH_3CCH	< 0.045
CH_2CO	< 0.032
CH_3CHO	< 0.025
c—C_2H_4O	< 0.20
C_2H_5OH	< 0.10
CH_3OCH_3	< 0.45
CH_3COOH	< 0.06
CH_2OHCHO	< 0.04
NH_2CH_2COOH	< 0.15
HC_5N	< 0.003
C_2H_5CN	< 0.010
CH_2NH	< 0.032
NH_2CN	< 0.004
NH_2OH	< 0.25
HCNO	< 0.0016
N_2O	< 0.23
NS	< 0.01

Molecule	[X]/[H_2O]
H_2CS	< 0.04
CH_3SH	< 0.05
NaOH	< 0.0003
NaCl	< 0.0008
PH_3	< 0.16
HDCO	< 0.05
CH_3OD	< 0.07
CH_2DOH	< 0.06
NH_2D	< 0.08
HDS	< 0.3

Table 7. Observed isotopic ratios (Compiled from [04B3] supplemented by [09M].)

Ratio	Molecule	Comet	Value
D/H	H_2O	1P/Halley	$(3.08^{+0.38}_{-0.53})\ 3 \times 10^{-4}$
	H_2O	1P/Halley	$(3.06 \pm 0.34) \times 10^{-4}$
	H_2O	C/ 1996 B2 (Hyakutake)	$(2.9 \pm 1.0) \times 10^{-4}$
	H_2O	C/1996 O1 (Hale-Bopp)	$(3.3 \pm 0.8) \times 10^{-4}$
	HCN	C/1996 O1 (Hale-Bopp)	$(2.3 \pm 0.4) \times 10^{-3}$
	H_2CO	1P/Halley	$< 2 \times 10^{-2}$
	H_2CO	C/1996 O1 (Hale-Bopp)	$< 5 \times 10^{-2}$
	CH_3OH	1P/Halley	$<\sim 1 \times 10^{-2}$
	CH_3OD	C/1996 O1 (Hale-Bopp)	$< 3 \times 10^{-2}$
	CH_2DOH	C/1996 O1 (Hale-Bopp)	$< 8 \times 10^{-3}$
	NH_3	C/ 1996 B2 (Hyakutake)	$< 6 \times 10^{-2}$
	NH_3	C/1996 O1 (Hale-Bopp)	$< 4 \times 10^{-2}$
	CH_4	153P/2002 C1	$< 1 \times 10^{-1}$
	H_2S	C/1996 O1 (Hale-Bopp)	$< 2 \times 10^{-1}$
	CH	C/ 1996 B2 (Hyakutake)	$< 3 \times 10^{-2}$
$^{12}C/^{13}C$	C_2	4 comets	93 ± 10
	CN	5 comets	90 ± 10
	CN	22 comets	91 ± 3.6
	HCN	C/ 1996 B2 (Hyakutake)	34 ± 12
	HCN	C/1996 O1 (Hale-Bopp)	111 ± 12
	HCN	C/1996 O1 (Hale-Bopp)	109 ± 22
	HCN	C/1996 O1 (Hale-Bopp)	90 ± 15
$^{14}N/^{15}N$	CN	22 comets	147.8 ± 5.7
	HCN	C/1996 O1 (Hale-Bopp)	323 ± 46
	HCN	C/1996 O1 (Hale-Bopp)	330 ± 98
	HCN	C/1996 O1 (Hale-Bopp)	138 – 239
	HCN	17P/Holmes	139 ± 26
$^{16}O/^{18}O$	H_2O	1P/Halley	518 ± 45
	H_2O	1P/Halley	470 ± 40
	H_2O	153P/2002 C1	450 ± 50
$^{32}S/^{34}S$	S^+	1P/Halley	23 ± 6
	CS	C/1996 O1 (Hale-Bopp)	27 ± 3
	H_2S	C/1996 O1 (Hale-Bopp)	17 ± 4

4.3.4.4 Measurements from space missions

Since 1985, eleven space encounters with comets have successfully been executed involving four space agencies – the European Space Agency (ESA), the Japan Aerospace Exploration Agency (JAXA), the National Aeronautics and Space Administration (NASA), and the Russian Federal Space Agency (Roskosmos) – and visiting six different short-period comets.

Six space missions visited comet 1P/Halley in 1986, of which three – the Japanese *Suisei* and *Sakigake* missions and the US American *International Cometary Explorer* (ICE) mission – were dedicated to explore the hydrogen corona, the plasma environment and its interaction with the solar wind at nucleus distances of the order of 10^5 - 10^7 km. The other three missions to comet 1P/Halley – the Russian *VeGa 1* and *VeGa 2* missions and the European *Giotto* mission – probed the near-nucleus environment and imaged the comet nucleus.

The ICE and the *Giotto* spacecraft each performed another comet fly-by returning data mainly on plasma and fields in the vicinity. In 1985, ICE went to comet 21P/Giacobini-Zinner, and the Giotto Extended Mission (GEM) had a close fly-by at 26P/Grigg-Skjellerup in 1992.

Between 2001 and 2005 three more comets were visited by NASA missions. The fly-by of the *Deep Space 1* probe at comet 19P/Borrelly in 2001 was followed in 2004 by the *Stardust* mission. *Stardust* performed a fly-by at comet 81P/Wild, at which coma dust particles were collected in an aerogel sampling container and successfully returned to Earth in January 2006 for laboratory analysis. In 2005 the *Deep Impact* mission to comet 9P/Tempel was executed, a fly-by mission impacting a heavy copper projectile with the comet nucleus to excavate a crater controlled by gravity.

Much of our knowledge about comets is based on the results of the measurements from these comet missions. The in-situ measurements of the near-nucleus and plasma environment have provided information not available through remote-sensing observations.

Table 8. Space missions to comets

Name	Target comet	Encounter date	Flyby distance [km]	
ICE	21P/Giacobini-Zinner	11 Sep 1985	7,800	[86V]
VeGa 1	1P/Halley	06 Mar 1986	8,890	[86S]
Suisei	1P/Halley	08 Mar 1986	1.5×10^5	[86H]
VeGa 2	1P/Halley	09 Mar 1986	8,030	[86S]
Sakigake	1P/Halley	11 Mar 1986	7×10^6	[86H]
Giotto	1P/Halley	14 Mar 1986	596	[86R]
ICE	1P/Halley	25 Mar 1986	2.8×10^7	[86B]
GEM	26P/GriggSkellerup	10 July 1992	< 200	[93G]
DS-1	19P/Borrelly	22 Sep 2001	2,170	[02S1]
Stardust	81P/Wild	02 Jan 2004	237	[04T]
Coma Dust Return (2nd part of Stardust)		15 Jan 2006	N/A	[06B2]
Deep Impact	9P/Tempel	04 Jul 2005	500	[05A]

4.3.4.5 Nucleus

A comet nucleus is a solid body, typically a few kilometres in size, composed of frozen gases and dust. The nucleus is the only component that is permanently present in a comet. It is the source of all comet activity phenomena, including coma and tails.

Dimensions, shape, rotation

The size of the nucleus is estimated mostly from CCD images of the comet obtained in the visible spectra range by measuring the Sunlight reflected from the nucleus and assuming a geometric albedo of 3 - 4%. The technique is most successful for relatively large and/or very low activity nuclei at large heliocentric

distance, and for comets observed at close range and with sufficient spatial resolution to separate unambiguously the nucleus and coma signals [04L1]. Radar detections are also possible if the nucleus is very large or passes very close to the Earth [04H2]. A third method is the in-situ imaging of the nucleus from spacecraft encounters (see 4.3.4.4). Reliable sizes have been determined for about 100 comets showing that comets mostly have kilometre-sized nuclei [04L1]; however there may be an observational bias for comets near the Earth [08H].

Comet nuclei generally show irregular, often elongated shapes with typical axis ratios (determined from rotational light curves) of about 2:1:1. (Strictly the light curve gives only the projection of the shape into the plane of the sky.) More accurate information on the nucleus shape is available for the four comet nuclei of which resolved images exist.

The nuclei of comets rotate with different spin periods, and in different, sometimes complex rotational states. Rotational parameters can be determined from (1) short-term variations in the light curve of a rotating elongated nucleus, (2) variations in the coma activity curve, (3) re-occurrence of prominent coma features, (4) patterns on the nucleus surface if the nucleus is resolved. About two dozen rotational rates of comet nuclei are known [97J, 00J, 04S1].

Albedo and colour

Comet nuclei are "black" with very low geometric albedo – defined as the zero-phase, disc-integrated reflectance relative to that produced by a "perfect" diffusing disc [81H]. The albedo is usually determined from parallel measurements of the optically scattered and thermally emitted fluxes. High albedo objects are optically bright, but thermally faint (cool); low albedo objects are optically dark, but thermally bright (they absorb most of the incident solar flux). Table 11 summarizes the results of albedo measurements of comet nuclei. For the four comet nuclei of which resolved images exist (1P/Halley, 9P/Tempel 1, 19P/Borrelly, 81P Wild 2) small albedo variations were observed over the surface of the nucleus.

As the incident Sunlight at optical wavelengths is reflected by the nucleus surface, the colour of a comet nucleus provides hints on surface composition and regolith particle size. In the optical broad band colour indices (B-V, V-R, R-I) are most commonly used for colour characterization. Colours are also discussed in terms of normalized reflectivity gradients $S' = dS/d\lambda / \langle S \rangle$, where S is the reflectivity (object flux density divided by solar flux density at same wavelength, λ) and $\langle S \rangle$ is the mean value of the reflectivity in the wavelength range over which $dS/d\lambda$ is computed. S' is used to express the percentage change in the strength of the reflected continuum light per 100 nm (%/100 nm). Broad band colour indices can be converted to normalized reflectivity gradients using

$$(V\text{-}R)_n = (V\text{-}R)_\odot + 2.5\log\,[(2+S'\Delta\lambda)/(2+S'\Delta\lambda)], \quad (4)$$

where $(V\text{-}R)_n$ and $(V\text{-}R)_\odot$ are the colour indices of the nucleus and the Sun respectively and $\Delta\lambda$ is the difference between the effective wavelengths of the two filters. Table 12 shows the measured colour indices of comet nuclei. The mean value of S' (%/100 nm) determined from observations of 12 comet nuclei is 8 ± 3. See [02J, 04L1] for reviews.

Table 9. Dimensions of comet nuclei determined from in-situ imaging

Comet	Dimensions	Ref.
1P/Halley	15.3 km × 7.2 km × 7.2 km	[87K, 90M]
9P/Tempel 1	7.6 km (max), 4.9 km (min)	[05A]
19P/Borrelly	8.0 km × 3.2 km × 3.2 km	[02S1]
81P Wild 2	5.5 km × 4.0 km × 3.3 km	[04B1]

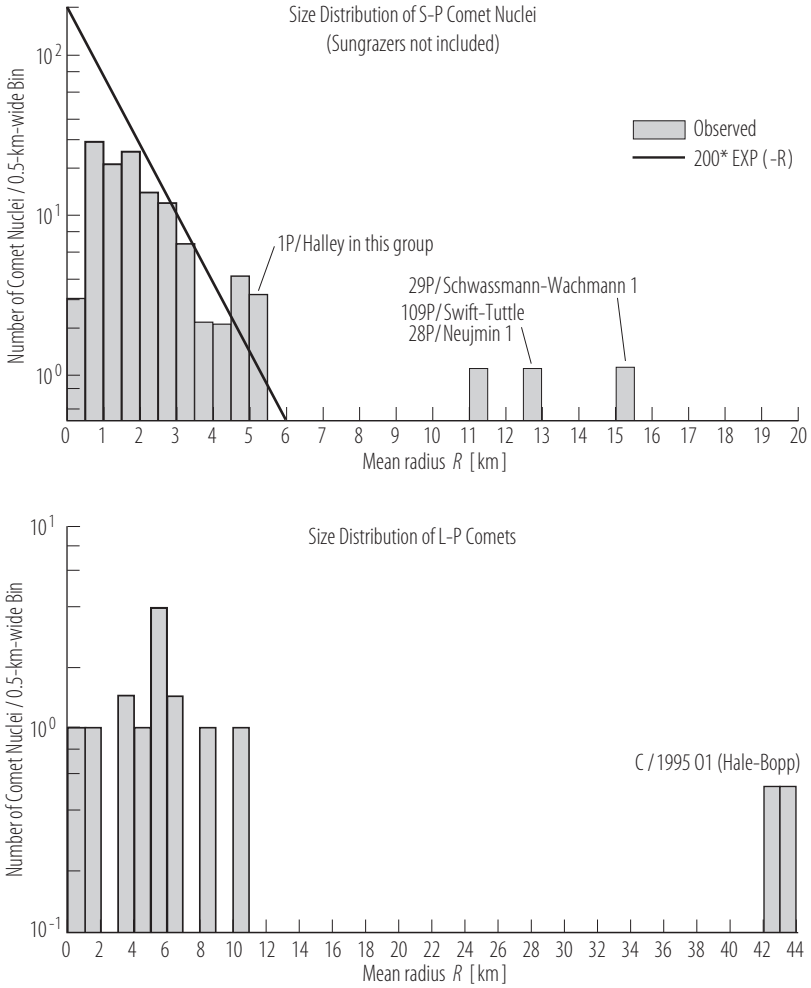

Fig. 5. Distribution of mean radii of short-period and long-period comet nuclei (from [08H]).

Table 10. Comet nucleus rotational periods (summarized from [00J, 04S1], supplemented with [07M])

Comet	Period(s) / hours	Method[1]
1P/Halley	175.2/88.6[2]	LC/SI/AV/JET
2P/Encke	15.08[3]	LC
6P/d'Arrest	7.2	LC
9P/Tempel 1	41	AV
10P/Tempel 2	8.93	LC
19P/Borrelly	26	LC
21P/Giacobini-Zinner	19	LC
22P/Kopff	12.3	LC
28P/Neujmin 1	12.67	LC
29P/Schwassmann-Wachmann 1	14.0/32.3[3]	LC
31P/Schwassmann-Wachmann 2	5.58	LC
46P/Wirtanen	6.0	LC
48P/Johnson	29	LC
49P/Arend-Rigaux	13.56	LC
95P/Chiron	5.9	LC
96P/Macholz	6.38	LC
107P/Wilson-Harrington	6.1	LC
109P/Swift-Tuttle	66.5	JET

Comet	Period(s) / hours	Method[1]
133P/Elst-Pizarro	3.47	LC
143PKowal-Mrkos	17.2	LC
C/1990 K1 (Levy)	8.94	LC
C/1991 L3 (Levy)	8.34	LC
C/1996 B2 (Hyakutake)	6.3	JET
C/1995 O1 (Hale-Bopp)	11.3	JET
C/1983 H1 (IRAS-Araki-Alcock)	51.4	LC

[1] LC = visual lightcurve, SI = spacecraft images, AV = activity variations, JET = dust or gas jet analysis.
[2] Non-principal spin state.
[3] Possible non-principal spin state.

Table 11. Geometric albedos of comet nuclei (Compiled from [04L1] supplemented by the authors.)

Comet	Geometric Albedo	Band or wavelengths [nm]
1P/Halley	$0.04^{+0.02}_{-0.01}$	V, R, I
2P/Encke	0.046 ± 0.023	V
9P/Tempel 1	0.04 ± 0.02	visible
10P/Tempel 2	$0.022^{+0.004}_{-0.006}$	484.5
10P/Tempel 2	0.04 - 0.07	JHK
19P/Borrelly	0.030 ± 0.005	visible
22P/Kopff	0.042 ± 0.006	V
28P/Neujmin 1	0.026	V
28P/Neujmin 1	0.03 ± 0.01	R
49P/Arend-Rigaux	0.04 ± 0.01	V
55P/Tempel-Tuttle	0.06 ± 0.025	R
67P/Churyumov-Gerasimenko	0.039-0.043	thermal IR
81P/Wild 2	0.03 ± 0.015	visible
107P/Wilson-Harrington	0.05 ± 0.01	J
109P/Swift-Tuttle	0.02 - 0.04	R
C/1983 H1 (IRAS-Araki-Alcock)	0.03 ± 0.01	V
C/1995 O1 (Hale-Bopp)	0.04 ± 0.03	
C/2001 OG108 (LONEOS)	0.03 ± 0.005	V

Table 12. Colour indices of comet nuclei (compiled from [04L1] supplemented by the authors.)

Comet	(B-V)	(V-R)	(R-I)
1P/Halley	0.72 ± 0.04	0.41 ± 0.03	0.39 ± 0.06
2P/Encke	0.78 ± 0.02	0.43 ± 0.05	-
6P/d'Arrest	0.78 ± 0.04	0.62 ± 0.08	0.45 ± 0.04
9P/Tempel 1	0.84 ± 0.01	0.50 ± 0.01	0.49 ± 0.02
10P/Tempel 2	-	0.56 ± 0.02	-
14P/Wolf	-	0.02 ± 0.22	0.25 ± 0.35
19P/Borrelly	-	0.25 ± 0.78	-
21P/Giacobini-Zinner	0.80 ± 0.03	0.50 ± 0.02	-
22P/Kopff	0.77 ± 0.05	0.50 ± 0.08	0.42 ± 0.03
28P/Neujmin 1	-	0.48 ± 0.06	-
45P/Honda-Mrkos-Pajdušáková	1.12 ± 0.03	0.44 ± 0.03	0.20 ± 0.03
46P/Wirtanen	-	0.45 ± 0.10	-
48P/Johnson	-	0.50 ± 0.30	-
49P/Arend-Rigaux	0.77 ± 0.03	0.49 ± 0.11	0.54 ± 0.14
53P/Van Biesbroeck	-	0.34 ± 0.08	-
73P/Schwassmann-Wachmann 3	-	0.48 ± 0.17	-
83P/Wild 3	-	0.12 ± 0.14	-

Comet	(B-V)	(V-R)	(R-I)
96P/Machholz 1	-	0.30 - 0.43	-
107P/Wilson-Harrington	0.61 - 0.75	0.20 - 0.41	-
133/Elst-Pizarro		0.14 ± 0.11	
143P/Kowal-Mrkos	0.82 ± 0.04	0.58 ± 0.02	0.56 ± 0.03
C/2001 OG108 (LONEOS)	0.76 ± 0.03	0.46 ± 0.02	0.44 ± 0.03
Solar colours	0.65	0.35	0.28

Temperature

The surface temperature of a comet nucleus depends on the albedo and vaporization rate. The steady state for a rotating nucleus can be described by

$$0.25\, F_0 (1 - A_v)\, r^{-2} = \sigma\, T^4 (1 - A_i) + Z(T) L(T), \tag{5}$$

where F_0 is the solar flux density at heliocentric distance r = 1 AU; A_v and A_i are mean albedos in the visible and infrared, T is the surface temperature, Z is the vaporization rate [molecules $m^{-2}s^{-1}$], L is the latent heat per molecule, and σ stands for the Stefan-Boltzmann constant. For Z = 0, the surface temperature $T \approx T_0\, r^{-1/2}$, where $T_0 \approx 280$ K if A_v and A_i are < 0.1. Diurnal temperature variations and heat conduction to the interior also play a role. The central temperature of a comet nucleus may partly be determined also by exothermic processes if some radioactive long-lived isotopes are present [91R, 04P].

Table 13. Measured surface temperatures of comet nuclei

Comet	Surface temperature [K]	Ref.
1P/Halley	> 360	[87E]
9P/Tempel 1	272 ± 7 to 363 ± 7	[07G]
19P/Borrelly	< 300 to 340	[04S4]
81P Wild 2		[04B1]

Structure, density, mass, and composition

Comet nuclei are solid, icy bodies composed of a mixture of frozen-gas ices, silicates, and organic materials. The classical "icy conglomerate" model proposed in 1950 [50W] is (in a modified version) still used as the basic model to explain their structure and composition.

Bulk density is estimated to lie between 0.3 - 1.2 gcm^{-3}, whereby values at the lower end are generally favoured [04W, 06H], but gas-to-dust ratio as well as porosity is poorly known. Mass is modelled from non-gravitational effects [93R, 04W]. Internal mass distribution is unknown. For discussions and references concerning the origin and early evolution of comet nuclei see [u].

The nucleus composition is usually approximated from measured composition of dust and gas coma assuming certain physico-chemical conditions in the near-nucleus region, where (photo)-chemical reactions take place. The dominant volatile is H_2O, followed by CO, CO_2 and several minor species present at the < 1% level. See reviews and discussions in [93R, 00H, 05C, 06H, 08H].

Physical processes in comet nuclei

A number of physical processes are relevant in the comet nucleus and at its surface for producing the phenomena describing a comet. Inside the nucleus the most important processes are: radiative heating, heat retention, heat and gas diffusion, crystallization of amorphous water ice (if present). Compressibility and tensile strength of nucleus material depend on the amount and type of sintering that is induced by thermal conduction. Close to the surface, sublimation and condensation of volatile ices, dust mantle formation and dust entrainment by escaping gases are important. Recent models and discussions [04P, 06H].

Split comet nuclei

Split comet nuclei usually appear as multiple objects with two or more components, initially moving in similar orbits. The phenomenon is known since 3D/Biela was observed as two pieces in 1846 and 1852, and then disappeared. One distinguishes tidally from non-tidally split comets. Non-tidal splitting is not understood, seems to occur at random and is often preceded by an outburst. Various fragmentation scenarios have been proposed. In few cases the nucleus of the same comet split repeatedly during (different) apparition(s). The Sun grazer comets or Kreutz Group has been identified as a family of split comets. Reviews of observations and theory [82S, 00B, 04B2]

Table 14. List of split comets, likely split pairs, and families of split comets. For periodic comets the year(s) of the splitting event is given in parenthesis. (Compiled from [04B2] supplemented by the authors)

Tidally split comets
C/1882 R1 (Great September Comet)
16P/Brooks 2 (1889 + 1995)
C/1963 R1 (Pereyra)
C/1965 S1 (Ikeya-Seki)
D/1993 F2 (Shoemaker-Levy 9) – Only secure case of tidally split comet.

Comets split for unknown reasons
3D/Biela (1840)
C/1860 D1 Liais)
C/1988 D1 (Sawerthal)
C/1889 O1 (Davidson)
205P/Giacobini = C/1896 R2 (Giacobini)
C/1899 E1 (Swift)
C/1906 E1 (Kopff)
C/1914 S1 (Campbell)
C/1915 C1 (Mellish)
69P/Taylor (1915)
C/1942 X1 (Whipple-Fedtke)
C/1947 X1 (Southern Comet)
C/1955 O1 (Honda)
C/1956 F1 (Wirtanen)
C/1968 U1 (Wild)
C/1969 O1 (Kohoutek)
C/1969 T1 (Tago-Sato-Kosaka)
C/1975 V1 (West)
79P/du-Toit-Hartley (1982)
108P/Ciffreo (1985)
C/1986 P1 (Wilson)
101P/Chernykh (1991)
C/1994 G1 (Takamaziwa-Levy)
141P/Machholz 2 (1987 + 1989)
51P/Harrington (1994 + 2001)
73P/Schwassmann-Wachmann 3 (1995/1996 + 2001 + 2006)
C/1996 B2 (Hyakutake)
C/1996 J1 (Evans-Drinkwater)
128P/Shoemaker-Holt (1996)
D/1999 S4 (LINEAR)
C/2001 A2 (LINEAR)
57P/du-Toit-Neujmin-Delporte (2002)
C/2003 S4 (LINEAR)

P/2004 V5 = P/2003 YM_{159} (LINEAR-Hill)
C/2004 S1 (Van Ness)
C/2004 U1 (LINEAR)
C/2005 A1 (LINEAR)
C/2005 K2 (LINEAR)

Likely split pairs
C/1988 F1 (Levy), C/1988 J1 (Shoemaker-Holt)
C/1988 A1 (Liller), C/1996 Q1 (Tabur)
C/2002 C1 (Ikeya-Zhang), C/1661 C1
C/2002 A1 (LINEAR), C/2002 A2 (LINEAR)
C/2002 Q2 (LINEAR), C/2002 Q3 (LINEAR)

Likely split families
42P/Neujmin 3, 53P/Van Biesbroeck, 14P/Wolf, 121P/Shoemaker-Holt 2
C/1965 S1 (Ikeya-Seki), C/1882 R1 (Great September Comet), C/1970 K1 (White-Ortiz-Olelli)
C/1880 C1 (Great Southern Comet), C/1843 D1 (Great March Comet)
Kreutz group and SOHO comets

4.3.4.6 Coma

Phenomenology:
The coma, also referred to as the comet atmosphere, is a gas-dust mixture surrounding the nucleus. Nucleus and coma make up the comet head.

A coma is newly formed from frozen volatiles sublimating off the nucleus and dragging dust particles with them (fountain model [10E]) each time the comet approaches the inner Solar System, and vanishes again during the post-perihelion phase when the comet moves away from the Sun.

The coma is not gravitationally bond to the nucleus, hence permanently diluting into space – therefore during its existence continuously replenished.

Brightness and extension of coma at fixed distance depend on size and activity of the nucleus (radius can reach several 10^5 km). Neutral gas coma appears almost circular; slight elliptic distortions are caused by solar radiation pressure. Observed gas expansion velocities are about 1 km/s^{-1} at r = 1 AU. The expansion velocity of the dust depends on the dust grains mass. Terminal velocities at r = 1 AU are about 100m s^{-1} for dust particles with mass 10^{-8} kg, and 1 km s^{-1} for all particles with mass < 10^{-13} kg. Dust coma generally less extended as dust particles move fast into dust tail (Sec. 4.3.4.7.).

Many comets exhibit discrete coma features (jets, fans, shells) detectable in gas and/or dust component. Some, but not all are connected to the rotational properties of the nucleus. [91S, 93F, 04S2, 02S3, 04C4]

Coma composition does not reflect nucleus composition, as material was altered by photochemical reactions and collisions, but plays important role for inferring the nucleus properties. In the gas coma parent species (molecules) released by sublimation from nucleus are distinguished from daughter species produced by photo-dissociation and/or -ionization processes. From radial distribution of parent and/or daughter species production and destruction mechanisms and lifetimes can be inferred. At heliocentric distance r = 1 AU the typical lifetimes are 10^4 s for parent molecules, and up to 10^5 s for daughter products [04R, 06S2].

Daughter products, i.e. radicals (such as OH, NH, CN, CH, C_3, C_2, NH_2) are observable in the optical and compose the visible coma. Parent molecules are observable at radio, IR and UV wavelengths. UV study is reduced to diatomic molecules (e.g. CO, CS, and S_2) and atoms. The atomic H coma is observable at Lyα and reaches dimensions of several 10^7 km. The coma is also detected in soft X-rays (E < 1 keV) [82A, 04F1, 04B3, 06C, 04L2].

Coma gas dynamics and kinetics plays an important role for the correct conversion of measured gas abundances into gas production rates. Review of available models in [04C2].

Ortho-to-para ratio

Molecules with more than one hydrogen atom may exist in different nuclear spin orientations according to the sum I of the spins of their hydrogen atoms. For molecules with two hydrogen atoms, such as water, the spins may be oriented in the same direction, called ortho ($I = 1$), or in opposite directions, called para ($I = 0$). Transitions between these two states are strictly forbidden. Therefore the ortho-to-para ratio can be related to the formation temperature of the comet nucleus. For discussion see [04B3].

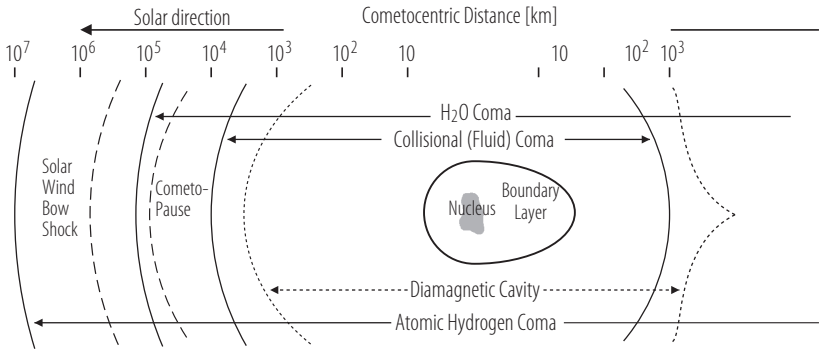

Fig. 6. Schematic illustration of the coma structure and its major physical regions for a moderate production rate at 1 AU. Note the logarithmic distance scale (from [04R]).

4.3.4.7 Tails

Today, three types of comet tails are known to exist. The traditionally known tails are the plasma (ion, type I) tail, and the dust (type II) tail. A third type of tail (type III) was discovered in 1997, detected in sodium emission [97C].

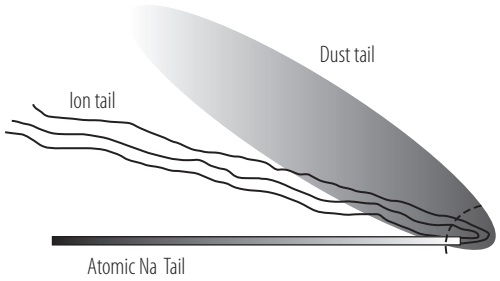

Fig. 7. A sketch showing the three tails in Comet C/1995 O1 (Hale-Bopp): Ion tail, dust tail, and sodium tail. The Sun is to the right, opposite the sodium tail. Modified from figure in [98I].

Plasma (ion, type I) tail

Interaction of ionized coma gas molecules with solar wind and interplanetary magnetic field manifests in a nearly straight, quasi anti-solar directed plasma tail, optically traceable to comet nucleus distances of some 10^8 km, with widths of typically 3000 - 4000 km. The main emission bands in the plasma tail are those of CO^+, N_2^+, H_2O^+, CO_2^+, CH^+, CN^+, and OH^+ [82W] with CO^+, N_2^+ having the longest lifetimes ($\tau \approx 10^6$ s). More recently, H_3O^+, HCO^+, O^+ and O^{3+} ions were discovered [99R, 07N].

For pioneering work on the plasma tail formation see [51B, 57A]. Recent reviews include the formation concepts of receding envelopes and ion-ray folding as well as progress in simulations of comet-solar wind interactions [04C3, 04I]. For the latest MHD models describing these interactions see [07H]. Correlations of plasma tail disturbances and disconnection events with solar wind events and crossings of comets and heliocentric current sheets are still under debate. The first direct observation of an interaction with a solar coronal mass ejection supports a magnetic origin for large-scale tail disconnections [07V].

In-situ measurements of particle and field instruments obtained during dedicated spacecraft encounters (see Sec. 4.3.4.4) resulted in the detection of different regions in the plasma boundary

structures developed by comet-solar wind interactions. Five regions were identified as a function of distance from the comet nucleus: (1) shock, (2) cometosheath, (3) cometopause, (4) ion pileup region, (5) magnetic field-free cavity.

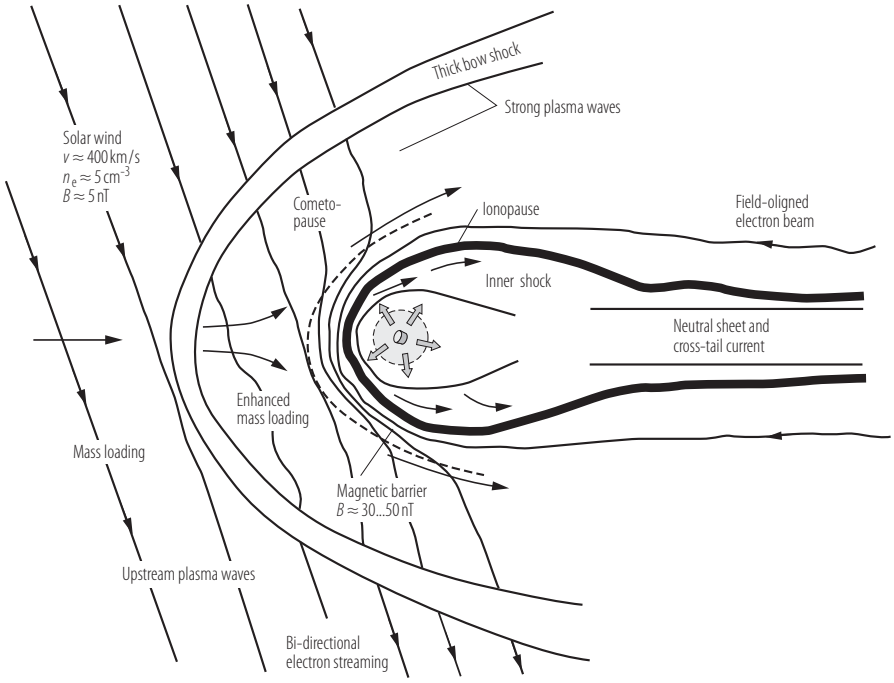

Fig. 8. Schematic picture of the plasma tail and solar wind-comet interaction.

Dust (type II) tail

The dust tail (typical length: 10^6km) is formed from grains of different sizes released from the comet nucleus into the coma and, once decoupled from the gas, moving on their own Keplerian orbits ($1/a = 1/|\vec{r}| - |\dot{\vec{r}}|/(\mu GM)$) around the Sun under the influence of solar gravity (F_{grav}) and solar radiation pressure (F_{rad}). Both forces act in the solar radial direction and are proportional to r^{-2}. With the reduced gravitational force on the particles defined as $\mu = (F_{grav} - F_{rad})/F_{grav}$ dust motion can be roughly defined by the radiation pressure parameter $\beta = (1-\mu)$ with $(1-\mu) < 1$: orbit concave (hyperbolic) to Sun; $(1-\mu) > 1$: convex; $(1-\mu) = 1$: straight line. β depends on particle properties. i.e. radius, density, and radiation pressure efficiency, and is independent on the distance from the Sun.

Mechanical theory initiated by [36B] and extended by [03B], explains dust tail formation and gross morphology based on the concept of synchrones and syndynes (or syndynames). Synchrones are almost straight lines on which grains released from the nucleus at a given time with zero initial velocity are located. Syndynes are the loci of dust particles ejected at different times but having the same $(1-\mu)$ and thus will experience the central force. Two-dimensional models were refined by a three dimensional model describing the dust tail to be built up by spherical dust shells and thus implying isotropic dust ejection [68F]. New approaches are based on Monte Carlo method. For a recent review see [04F2].

Repulsive force of the radiation pressure causes the dust tail to be located outside the comet orbit and behind the orbital plane.

An anti-tail (or anomalous tail), sometimes observed as a part of the comet tail, but apparently pointing towards the Sun, results from observational projection effect, based on given comet-Sun-Earth position. Anti-tail is composed of heavy dust particles of the order of ~ 0.01 - 0.1 cm [76S]. Heavy grains have small β values and stay longer in nucleus vicinity, whereas smaller particles have moved far away and are no longer visible.

A neck-line is composed of large grains (> cm) ejected at true anomaly of 180° (first node) away from the observation point (second node) [77K]. The initially spherical dust shell, w.r.t. Finson-Probstein

model ([68F]), which is ejected isotropically from the nucleus before perihelion, will collapse on the comet orbital plane at the second node, becoming a 2D ellipse. When the Earth crosses the comet orbit, an extended straight narrow line is observed that is brighter than the surrounding dust tail.

An anti-neck-line is a particular type of anti-tail discovered by [87P]. They are the part of the 2D ellipse forming the neck-line that is located inside the comet orbit ahead of the nucleus with respect to the Sun. They contain the largest grains and can reach a length of $\leq 10^6$km.

Dust tails sometimes contain inhomogeneities, so-called streamers and striae. Streamers are produced by particles of different sizes expelled simultaneously from the nucleus (synchrones) either as a consequence of varying dust emission activity [78S] or nucleus rotation with an anisotropic distribution of dust sources [80S]. Striae are created as daughter products due to fragmentation of larger grains [92B]. Thus they are synchrones, but originating from the point in the tail where the parent grain was located at the time of fragmentation.

The dust tail is morphological diffuse and appears generally white because of scattered Sunlight within a wavelengths range of 400 - 600 nm by dust grains sizes of roughly of 1 to 10 μm. The observed brightness is a result of the higher scattering efficiencies of these particles in wavelength range and the decreasing number density versus increasing particles size [04K]. The number density is defined by the particle size distribution, $f(a)$, which is commonly assumed to follow a power index with $f(a) = a^{-\alpha}$.

The cometary dust is mainly composed of rock-forming minerals (Mg, Si, Ca, Fe) and organic refractory material (H, C, N, O) whereas silicates, present in crystalline and amorphous form, constitute the most abundant material [04H1].

Neutral gas (sodium, type III) tail

The sodium tail discovered in Comet Hale-Bopp [97C] displays a third type of tail approximately 600,000 km wide and 50 million km long pointing into a direction close, but slightly different to that of the ion tail. It is formed by radiation pressure on the sodium.

The origin of the sodium is not yet fully explained. Sodium atoms may be released from very small dust grains or molecules emitted from the comet nucleus. Collisional interaction between micron-sized and very small dust grains (10 - 100 Å) has been suggested [98I].

4.3.4.8 The nature of cometary dust

The solid component of a comet, usually called “cometary dust”, is an un-equilibrated non-homogeneous mixture of crystalline and amorphous silicates, organic material and other minor constituents (e.g. iron sulphide, iron oxide, and Calcium-Aluminium minerals). It contains high and low temperature condensates, testifying the presence of a mixing in the pre-solar nebula, before the comet formation [02B3]. Probably a mix of grains with interstellar origin and others produced or transformed in proto-planetary disk. Once released from comet nucleus, it is not significantly altered by solar radiation. Recent reviews: [04H1, 04E, 04S3, 08W].

Measurements of composition and structure

Information is available from remote observations, in-situ measurements during comet fly-bys, and stratospheric collecting of Interplanetary Dust Particles (IDPs). One coma dust sample returned to Earth (Stardust, see [08S2] for a summary of results).

Remote observations have been obtained mainly at thermal-IR to detect silicates emitting at 10 μm (stretching vibrations of Si-O bonds). The emission is coming from grains < 1 μm or if bigger, very porous grains. Most information available for comet C/1995 OI (Hale-Bopp) which has been observed from ground and space (Infrared Space Observatory, ISO). Important measurements also of ejecta have been produced by Deep Impact mission to comet 9P/Tempel [05H].

In-situ measurements available for two comets: 1P/Halley (Giotto Mission), 81P/Wild 2 (Stardust Mission), see 4.3.4.4.

IDPs collected from stratospheric airplanes are very porous, fine grain aggregates (0.1 - 0.5 μm) with compositions similar to chondrite meteorites. Some may originate from comets.

Refractory grains

Are composed of "rocky" elements: C, O, Mg, Al, Si, S and Fe. Main components: amorphous silicates (olivine, pyroxene), and crystalline silicates rich in Mg, (olivine, fosterite, pyroxene, enstatite), amorphous carbon. Minor components: Fe-rich crystalline silicates, Calcium-Aluminium minerals, Iron-Nickel sulphide. Calcium-Aluminium Inclusions discovered by Stardust mission [06B1].

Crystalline and amorphous silicates are obvious in many near-isotropic comets, but barely detected in Jupiter-family comets [82C, 89G, 00C]. Only for 9P/Tempel during the Deep Impact mission both silicate types were well detected 1 h after the impact [05H]. Hence, because of their frequent perihelion passages, Jupiter-family comets may have a lower abundance of small grains, which are the first to be dispersed by an active comet into the interplanetary medium.

In comet C/1995 O1 (Hale-Bopp) small grains were mainly constituted of glassy pyroxenes (> 40%) and crystalline olivine (< 20%) [00H]. Amorphous carbon: 8 - 10% of the comet nuclei by mass.

Sublimating organic grains

Discovered in-situ in comet 1P/Halley and named CHON particles, a dust component predominantly composed of the light elements Carbon, Hydrogen, Oxygen, Nitrogen, most likely present as large organic compounds [86K1, 86K2]. Represent one explanation for so called "extended" or "distributed" sources of gaseous molecules (or radicals). Suggested processes are sublimation, photon-induced desorption, and photo-sputtering from grains or large polymerized molecules. Recent review in [08C].

Table 15. Comparison of element ratios (normalized to Mg = 100) in grains measured in comet and CI chondrites (from [08S2]).

Element	81P/Wild 2 (Aerogel)	81P/Wild 2 (Al foil)	1P/Halley	CI chondites
Li	0.0096	0.015		0.0053
Na	13	20	10	5.3
Mg	100	100	100	100
Al	16		6.8	7.9
Si		71	185	93
P		0.17		0.97
S	7.9	3.7	72	48
K	2.9	1.6	0.2	0.35
Ca	2.8	6.0	6.3	5.7
Sc	0.0093	0.0089		0.0032
Ti	0.34	0.12	0.4	0.22
V	0.0031			0.0027
Cr	1.3	0.48	0.9	1.26
Mn	0.80	0.49	0.5	0.89
Fe	81	18	52	84
Co	0.45	0.15	0.3	0.21
Ni	5.2	2.1	4.1	4.6
Cu	0.12			0.049
Zn	0.15			0.117
Ga	0.011			0.0035

Table 16. Relative mineralogy of comets by mass of submicron grains (from [06K]).

Comet	r [AU]	Amorphous carbon	Amorphous olivine	Amorphous pyroxene	Crystalline olivine	Silicate/ carbon
2P/Encke	2.6	$1.00^{+0.00}_{-0.07}$	< 0.01	< 0.14	< 0.05	< 0.08
C/2001 HT50 (LINEAR-NEAT)	3.2	$0.63^{+0.01}_{-0.05}$	$0.032^{+0.012}_{-0.004}$	< 0.006	$0.34^{+0.05}_{-0.02}$	$0.59^{+0.14}_{-0.04}$
C/2001 HT50 (LINEAR-NEAT)	4.6	$0.82^{+0.04}_{-0.25}$	$0.18^{+0.11}_{-0.08}$	< 0.14	< 0.60	< 2.2
C/1995 O1 (Hale-Bopp)	2.8	0.11	0.18	0.18	0.48	8.1
9P/Tempel 1 (pre-DI)[a]	1.5	0.0	1.0	0.0	0.0	…
9P/Tempel 1 (DI+1.0)[b]	1.5	0.21	0.27	0.41	0.10	3.7

[a]Before deep impact on comet nucleus
[b]Time of impact +1.0 h.

4.3.4.9 Laboratory studies relevant to comets

Laboratory studies of comet analogue materials provide quantitative information applicable for interpretation of remote and/or in-situ observations of comets. Numerous experiments have been performed over the last 25 years.

Comet simulation experiments usually involve (cold) sample preparation, subsequent irradiation, electrical heating, or charged particle bombardment, and pre- and post analysis. First comet simulation experiments by [67K].

Small samples are produced by condensation of vapour mixtures on cold fingers and thin films. Larger samples are produced by spraying techniques. Irradiation by UV photons, solar simulators, or ion irradiation (bombardment) of ices and ice mixtures lead to structural modification, textural changes, formation of new species, and erosion of materials. For reviews see [82G, 98J, 98S2, 99S, 01M, 04C1, 06H]

Table 17. Products from reactions of one-component ices and H_2O-dominated two-component ices at 10 - 20 K (from [04C1])

Ice	Products identified	Mixture	Products identified
H_2O	H_2O_2, HO_2, OH		
CO	CO_2, C_3O_2, C_2O	H_2O + CO	CO_2, HCO, H_2CO, CH_3OH, H_2CO_3, HCOOH, $HCOO^-$
CO_2	CO, CO_3, O_3	H_2O + CO_2	CO, H_2CO_3, O_3, H_2O_2
CH_4	C_2H_2, C_2H_4, C_2H_6, C_3H_8, CH_3, C_2H_5	H_2O + CH_4	CH_3OH, C_2H_5OH, C_2H_6, CO, CO_2
C_2H_2	CH_4, polyacetylen	H_2O + C_2H_2	C_2H_5OH, CH_3OH, C_2H_6, C_2H_4, C_3H_8, $HC(=O)CH_3$, CH_2CHOH, CH_4, CO_2, CO
C_2H_6	-	H_2O + C_2H_6	CH_4, C_2H_4, CH_3CH_2OH, CO_2, CH_3OH
H_2CO	POM, CO, CO_2, CHO	H_2O + H_2CO	CO_2, CO, CH_3OH, HCO, HCOOH, CH_4
CH_3OH	CH_4, CO_2, CO, H_2CO, H_2O, $C_2H_4(OH)_2$, HCO, $HCOO^-$	H_2O + CH_3OH	CO_2, CO, H_2CO, HCO, CH_4, $HCOO^-$, $C_2H_4(OH)_2$
NH_3	N_2H_4, NH_2	H_2O + NH_3	None reported
HCN	HCN oligomers	H_2O + HCN	CN^-, HNCO, OCN^-,

Ice	Products identified	Mixture	Products identified
			$HC(=O)NH_2$, CO, CO_2, NH_4^+(?)
HNCO	NH_4^+, OCN^-, CO, CO_2	H_2O + HNCO	NH_4^+, OCN^-, CO, CO_2
HCOOH	-	H_2O + HCOOH	CO_2, CO, H_2CO
$HC(=O)CH_3$	-	H_2O + $HC(=O)CH_3$	CO_2, CO, CH_4, CH_3CH_2OH
$HC(=O)NH_2$	-	H_2O + $HC(=O)NH_2$	CO_2, CO, HNCO, OCN^-
$HC(=O)OCH_3$	-	H_2O + $HC(=O)OCH_3$	CO_2, CO, H_2CO, CH_3OH, CH_4
SO_2	SO_3	H_2O + SO_2	-
H_2S	None reported	H_2O + H_2S	S_2
OCS	-	H_2O + OCS	
CH_3CN	CH_4, H_2CCNH, CH_3NC	H_2O + CH_3CN	H_2CCNH, CH_4, OCN^-, CN^-

Acknowledgement

We thank Ho Tra-Mi for her help in compiling section 4.3.4.7.

4.3.4.10 References for 4.3.4

Proceedings and monographs
(In special references referred to as Proceedings)

a Comets (Wilkening, l.l. ed.) Tucson: University of Arizona Press (1982)
b Nature **321** (1986) May, special issue (Space Missions to Comet Halley)
c Science **232** (1986) April 18, special issue (ICE Mission to Comet Giacobini-Zinner)
d Physics and Chemistry of Comets (Huebner, W.F., ed.) Heidelberg, Springer-Verlag (1990)
e Comets in the Post-Halley Era Vols. 1 & 2 (Newburn, R. L., Jr., Neugebauer, M., Rahe, J., eds.) Dordrecht, The Netherlands, Kluwer Academic Publishers (1991)
f Journal of Geophysical Research **98** (1993) – special issue (Giotto's Encounter with Comet Grigg-Skjellerup)
g Asteroids, Comets, and Meteors – ACM93, IAU Symposium **160** (Milani, A., di Martino, M., Cellino, A., eds.) Kluwer Academic Publishers (1993)
h Completing the Inventory of the Solar System (Rettig, T., Hahn, J.M., eds.) Astronomical Society of the Pacific Conference Proceedings **107** (1996)
i Earth, Moon, and Planets **79**, Nos. 1-3, Special Issue on 1st Hale-Bopp Conference, (A'Hearn, M.F., Boehnhardt, H., Kidger, M., West, R.M., eds.) Dordrecht/ Boston/ London, Kluwer Academic Publishers (1997)
j Solar System Ices (Schmitt, B., de Bergh, C., Festou, M., eds.) Kluwer Academic Publishers, Netherlands (1998)
k Earth, Moon, and Planets **89**, Nos. 1-4, Special Issue on Cometary Science after Hale-Bopp, (Boehnhardt, H., Combi, M., Kidger, M.R., Schulz, R., eds.) Dordrecht/ Boston/ London, Kluwer Academic Publishers (2000)
l Asteroids, Comets, Meteors - ACM 2002, ESA SP-**500**, (Barbara Warmbein ed.). Noordwijk, The Netherlands, ESA Publication, ISBN 92-9092-810-7 (2002)
m Science **304** (2004) June 18, special issue (Stardust at Comet Wild 2)
n Comets II, (Festou, M.C., Keller, H.U., Weaver, H.A., eds.), University of Arizona Press, Tucson (2004)
o Catalogue of cometary orbits, 16th edn. (Marsden, B.G., Williams, G.V.) Smithonian Astrophysical Observatory, Cambridge (2005)
p Science **310** (2005) October 14, special issue (Deep Impact)

q Asteroids, Comets, and Meteors – ACM 2005, IAU Symposium **229** (Lazzaro, D., Ferraz-Mello, S., Fernández, J., A., eds.) Cambridge University Press (2006)
r Heat and Gas Diffusion in Comet Nuclei (Huebner, W.F. Benkhoff, J., Capria, M.-T., Coradini, A., De Sanctis, C., Orosei, R., Prialnik, D.) ISSI Scientific Report, SR-004, ISBN: 1608-280X (2006)
s Science **314** (2006) December 15, special issue (Stardust)
t Deep Impact at Comet Temple 1 (A'Hearn, M.F., Combi, M.R., eds.) Icarus **191**, No. 2S (2007)
u Origin and Early Evolution of Comet Nuclei (H. Balsiger, K. Altwegg, W. Huebner, T. Owen, R. Schulz, eds.) Space Science Reviews **138**, Nos. 1-4 (2008)

Special references

36B Bessel, F.W.: Astronomische Nachrichten **13** (1836) 185.
03B Bredikhin, T., see Jaegermann: Kometenformen, St. Petersburg (1903).
10E Eddington, A.S.: MNRAS **70** (1910) 442.
43E Edgeworth, K.E.: Journal Brit. Astron. Soc. **53** (1943) 618.
49E Edgeworth, K.E.: MNRAS **109** (1949) 600.
50O Oort, J.H.: Bulletin Astron. Inst. Neth. **11** (1950) 91.
50W Whipple, F.L.: Astrophyical Journal **111** (1950) 375.
51B Biermann, L.: Zeitschrift für Astrophysik **29** (1951) 274.
51K Kuiper, G.P.: Astrophysics (Hynek, J.A., ed.) McGraw-Hill, New York (1951) p. 357.
57A Alfvén, H.: Tellus **9** (1957) 92.
67K Kajmakov, E.A., Sharkov, V.I.: Komety I Meteory **15** (1967) 16.
68F Finson, M.L., Probstein, R.F.: Astrophysical Journal **154** (1968) 327.
76S Sekanina, Z.: IAU Colloq. No **25 –** NASA SP-**393** (1976) 893.
77K Kimura, H., Liu, C.P.: Chinese Astron., **1** (1977) 235.
78S Sekanina, Z., Farrell, J.A.: Astron. J. **83** (1978) 1675.
80S Sekanina, Z., Farrell, J.A.: Astron. J. **85** (1980) 1538.
81H Hanner, M.S.: Astronomy and Astrophysics **104** (1981) 42.
82A A'Hearn, M.F.: see Proceedings [a] p.433.
82C Campins, H., et al.: Icarus **51** (1982) 461.
82F Feldman, P.D.: see Proceedings [a] p. 461.
82G Greenberg, J.M.: see Proceedings [a] p. 131.
82S Sekanina, Z.: see Proceedings [a] p. 251.
82W Wykoff, S.: see Proceedings [a] p. 3.
84A1 A'Hearn, M.F. et al.: Astron. J. **89** (1984) 579.
84A2 A'Hearn, M.F. et al.: International Halley Watch Letter No. **4** (1984) 21.
86B Brandt, J.C.: ESA SP-**1066** (1986) 99.
86H Hirao, K., Itoh, T.: Nature **321** (1986) 294.
86K1 Kissel, J. et al.: Nature **321** (1986) 280.
86K2 Kissel, J. et al.: Nature **321** (1986) 336.
86R Reinhard, R.: Nature **321** (1986) 313.
86S Sagdeev, R.Z. et al.: Nature **321** (1986) 259.
86V Von Rosenvinge, T.T., et al.: Science **232** (1986) 353.
87C Carusi, A., Valsecchi, G. B.: Publications of the Astronomical Institute of the Czechoslovak Academy of Sciences **67** (1987) 21.
87E Emerich, C. et al.: Astronomy and Astrophysics **187** (1987) 839.
87K Keller, H.U. et al.: Astronomy and Astrophysics **187** (1987) 807.
87P Pansecchi, L. et al.: Astron. Astrophys. **176** (1987) 358.
89G Gehrz, R.D. et al.: Icarus **80** (1989) 280.
90M Merényi, E. et al: Icarus **86** (1990) 9.
90O Osborn, W.H. et al.: Icarus **88** (1990) 228.
91L Larson, S.M. et al.: see Proceedings [e] p. 209.
91R Rickman, H.: see Proceedings [e] p. 733.
91S Sekanina, Z.: see Proceedings [e] p. 769.

92B Beisser, K., Drechsler, H.: Astrophys. Space Sci. **191** (1992) 1.
93F Festou, M.C., et al.: Astron. Astrophys. Review **4**, No. 4 (1993) 363.
93G Grensemann, M.G., Schwehm, G.: J. Geophys. Res. **98** (1993) 907.
93R Rickman, H.: see Proceedings [g] p. 297.
95M1 Marsden, B.G.: International Comet Quarterly **17** (1995) 3.
95M2 Marsden, B.G.: IAU Circular **6124** (1995) 2.
96L1 Levasseur-Regourd, A. C. et al.: Astron. Astrophys. **313** (1996) 327.
96L2 Levison, H.F.: see Proceedings [h] p. 173.
96S Schulz, R., Schwehm, G.: Planet. Space Sci. **44** (1996) 619.
97B1 Biver, N. et al.: Science **275** (1997) 1915.
97B2 Biver, N. et al.: EMP **78** (1997) 5.
97C Cremonese, G. et al.: Astrophysical Journal **490** (1997) L199.
97J Jewitt, D.: see Proceedings [i] p. 35.
97S Schleicher, D.G et al.: Science **275** (1997) 1913.
98I Ip, W.-H., Jorda, L.: Astrophysical Journal **496** (1998) L47.
98J Johnson, R.E.: see Proceedings [j] p. 30.
98S1 Schleicher, D.G. et al.: Icarus **132** (1998) 397.
98S2 Strazzulla, G.: see Proceedings [j] p. 281.
98S3 Schulz, R. et al.: Astron. Astrophys. **335** (1998) L46.
99K Kiselev, N.N.: Space Science Reviews **33** (1999) 158.
99R Rauer, H.: Earth, Moon Planets **79** (1999) 161.
99S Sears, D.W. et al.: Meteoritics & Planetary Science **34** (1999) 497.
00B Boehnhardt, H.: see Proceedings [k] p. 91.
00C Crovisier, J., et al.: Astron. Soc. Pacific Conf. Ser. **196** (2000) 109.
00F Farnham, T.L. et al.: Icarus **147** (2000) 180.
00H Huebner, H.: see Proceedings [k] p. 179.
00J Jorda, L., Gutiérrez, P.: see Proceedings [k] p. 135.
01F Farnham, T.L. et al.: Science **292** (2001) 134.
01M Moore, M.H. et al.: Spectrochim. Acta **A57** (2001) 841.
01S Strazzulla, G. et al.: Spectrochim. Acta **A57** (2001) 825.
02B1 Biver, N. et al.: Earth Moon Planets **90** (2002) 5.
02B2 Biver, N. et al.: Earth Moon Planets **90** (2002) 323.
02B3 Bockelée-Morvan, D. et al.: Astron. Astrophys. **384** (2002) 1107.
02C Crovisier, J. et al.: Astron. Astrophys. **393** (2002) 1053.
02J Jewitt, D.: see Proceedings [l] p. 11.
02M Muinonen, K. et al.: Asteroids III, Univ. Ariz. Press, Tucson,123.
02S1 Soderblom, L.A. et al.: Science **296** (2002) 1087.
02S2 Schleicher, D.G., Osip, D.J.: Icarus **159** (2002) 210.
03S Schleicher, D.G. et al.: Icarus **162** (2003) 415.
02S3 Schulz, R.: see Proceedings [l] p. 553.
04B1 Brownlee, D.E. et al.: Science **304** (2004) 1764.
04B2 Boehnhardt, H.: see Proceedings [n] p. 301.
04B3 Bockelée-Morvan, D. et al.: see Proceedings [n] p. 391.
04C1 Colangeli, L. et al: see Proceedings [n] p. 695.
04C2 Combi, M.R. et al.: see Proceedings [n] p. 523.
04C3 Cravens, T.E., Gombosi, T.I.: Adv. Space Res. **33** (2004) 1968.
04C4 Crifo, J.F. et al: see Proceedings [n] p. 471.
04C5 Crovisier, J. et al.: Astron. Astrophys. **418** (2004) 1141.
04D1 Dones, L. et al.: see Proceedings [n] p. 153.
04D2 Duncan, M. et al.: see Proceedings [n] p. 193.
04E Ehrenfreund, P. et al.: see Proceedings [n] p. 115.
04F1 Feldman, P.D. et al.: see Proceedings [n] p. 425.
04F2 Fulle, M.: see Proceedings [n] p.565.
04H1 Hanner, M., Bradley, J.P.: see Proceedings [n] p. 555.

04H2 Harmon, J.K. et al.: see Proceedings [n] p. 265.
04I Ip, W.-H.: see Proceedings [n] p. 605.
04K Kolokolova, L. et al.: see Proceedings [n] p. 577.
04L1 Lamy, P.L. et al.: see Proceedings [n] p. 223.
04L2 Lisse, C.M. et al.: see Proceedings [n] p. 631.
04M Morbidelli , A., Brown, M.E.: see Proceedings [n] p. 175.
04P Prialnik, D., et al.: see Proceedings [n] p. 359.
04R Rodgers, S.D., et al.: see Proceedings [n] p. 505
04S1 Samarasinha, N.H. et al.: see Proceedings [n] p. 281.
04S2 Schleicher, D.G., Farnham, T.L.: see Proceedings [n] p. 449.
04S3 Sykes, M.V. et al.: see Proceedings [n] p. 677.
04S4 Soderblom, L.A. et al.: Icarus **167** (2004) 100.
04T Tsou, P. et al.: J. Geophys. Res. **109** (2004) E12S01.
04W Weissman, P.R. et al.: see Proceedings [n] p. 337.
04Y Yeomans, D.K. et al.: see Proceedings [n] p. 137.
05A A'Hearn, M.F. et al.: Science **310** (2005) 258.
05C Crovisier, J.: see Proceedings [q] p. 133.
05F Farnham, T.L., Schleicher, D.G.: Icarus **173** (2005) 533.
05H Harker, D. E., et al.: Science **310** (2005) 278.
05J Jockers, K. et al.: Astron. Astrophys. **441** (2005) 773.
05M1 Marsden, B.G., Williams, G.V.: see Proceedings [o].
05M2 Marsden, B.G.: Ann. Rev. Astron. Astrophys. **43** (1995) 75.
05S Sekanina, Z., Chodas, P.W.: Astrophys. J. **161** (2005) 551.
06B1 Brownlee, D. et al.: Science **314** (2006) 1711.
06B2 Burnett, D.S.: Science **314** (2006) 1709.
06C Crovisier, J.: see Proceedings [q] p. 133.
06H Huebner, W.F.: see Proceedings [r] p. 18.
06K Kelley, M.S. et al.: Astrophys. J. **651** (2006) 1256.
06S1 Schleicher, D.G.: Icarus **181** (2006) 441.
06S2 Schulz, R.: see Proceedings [q] p. 413.
07B1 Bhardwaj, A. et al.: Planet. Space Sci. **55** (2007)1135.
07B2 Biver, N. et al.: Planet. Space Sci. **55** (2007)1058.
07C Campins, H. et al.: Astron. J. **134** (2007) 1626.
07G Groussin, O. et al.: Icarus **191** (2007) 63.
07H Hansen, K.C. et al.: Space Science Reviews **128** (2007) 133.
07L Landi Degl'Innocenti, E. et al.: ASP Conference Series **364** (2007) 495.
07M Manfroid, J. et al.: Icarus **191** (2007) 348.
07N Neugebauer, M. et al.: Astrophysical Journal **667** (2007) 1262.
07V Vourlidas, A.D.C. et al.: Astrophysical Journal **668** (2007) L79.
07S1 Schleicher, D.G.: Icarus **190** (2007) 460.
07S2 Sekanina, Z., Chodas, P.W.: Astrophys. J. **663** (2007) 657.
08B1 Boehnhardt, H. et al.: Astron. Astrophys. **489** (2008) 1337.
08B2 Bagnulo, S. et al.: Astron. Astrophys. **491** (2008) L33.
08C Cottin, H., Fray, N.: see Proceedings [u] p. 179.
08D Duncan, M.J.: see Proceedings [u] p. 109.
08H Huebner, W.F.: see Proceedings [u] p. 5.
08S1 Schleicher, D.G.: Astron. J. **136** (2008) 2204.
08S2 Stephan, T.: see Proceedings [u] p. 247.
08W Wooden, D.H.: see Proceedings [u] p. 75.
09M Manfroid, J. et al.: Astron. Astrophys. (2009) in press.